View metadata, citation and similar papers at core.ac.uk
brought to you by CORE
provided by Institutional Research Information System University of Turin

Rainfall as primary driver of discharge and solute export from rock glaciers: the Col d'Olen Rock Glacier in the NW Italian Alps

Nicola Colombo[1,2], Stephan Gruber[2], Maria Martin[3], Mery Malandrino[4], Andrea Magnani[3], Danilo Godone[5], Michele Freppaz[3], Simona Fratianni[1], Franco Salerno[6]

[1] University of Turin, Department of Earth Sciences, Via Valperga Caluso, 35, 10125, Turin, Italy

[2] Carleton University, Department of Geography and Environmental Studies, 1125 Colonel By Drive, Ottawa, ON, K1S 5B6, Canada

[3] University of Turin, Department of Agricultural, Forest and Food Sciences, Largo Paolo Braccini, 2, 10095, Grugliasco, Italy

[4] University of Turin, Department of Chemistry, Via Pietro Giuria, 5, 10125, Turin, Italy

[5] CNR-IRPI (National Research Council - Research Institute for Geo-Hydrological Protection), Strada delle Cacce, 73, 10135, Turin, Italy

[6] CNR-IRSA (National Research Council - Water Research Institute), Via del Mulino, 19, 20047, Brugherio, Italy

Correspondence to: nicola.colombo@unito.it

Abstract

Three hypotheses exist to explain how meteorological variables drive the amount and concentration of solute-enriched water from rock glaciers: (1) Warm periods cause increased subsurface ice melt, which releases solutes; (2) rain periods and the melt of long-lasting snow enhance dilution of rock-glacier outflows; and (3) percolation of rain through rock glaciers facilitates the export of solutes, causing an opposite effect as that described in hypothesis (2). This lack of detailed understanding likely exists because suitable studies of meteorological variables, hydrologic processes and chemical characteristics of water bodies downstream from rock glaciers are unavailable. In this study, a rock-glacier pond in the North-Western Italian Alps was studied on a weekly basis for the ice-free seasons 2014 and 2015 by observing the meteorological variables (air temperature, snowmelt, rainfall) assumed to drive the export of solute-enriched waters from the rock glacier and the hydrochemical response of the pond (water temperature as a proxy of rock-glacier discharge,

stable water isotopes, major ions and selected trace elements). An intra-seasonal pattern of increasing solute export associated with higher rock-glacier discharge was found. Specifically, rainfall, after the winter snowpack depletion and prolonged periods of atmospheric temperature above 0 °C, was found to be the primary driver of solute export from the rock glacier during the ice-free season. This occurs likely through the flushing of isotopically- and geochemically-enriched icemelt, causing concomitant increases in the rock-glacier discharge and the solute export (SO_4^{2-}, Mg^{2+}, Ca^{2+}, Ni, Mn, Co). Moreover, flushing of microbially-active sediments can cause increases in NO_3^- export.

1. Introduction

Permafrost degradation has been reported to impact the chemical characteristics of surface fresh water across the globe (Frey and McClelland, 2009; Vonk et al., 2015; Colombo et al., 2018a). Active rock glaciers are considered indicators of ice-rich permafrost in mountainous environments (for a review: Haeberli et al., 2006). Tens of thousands of rock glaciers are estimated to exist worldwide (Barsch, 1996) and their water storage may be hydrologically significant in some areas and times (Jones et al., 2018). Recently, increases in electrical conductivity and solute concentrations have been found in some rock-glacier lakes in the European Alps (Thies et al., 2007; Ilyashuk et al., 2014, 2017) and in the outflow of a rock glacier in the Colorado Front Range (Williams et al., 2006). Similar evidence was reported from some Himalayan lakes over the past two decades, where significant enrichment in solutes has been attributed to the retreat of debris-covered glaciers (Salerno et al., 2016). In all these cases, the authors consider air temperature as the main climatic driver of change and hypothesise on underlying physical processes. Thies et al. (2013) also reported that rock-glacier outflows can be highly enriched in heavy metals. Seasonally, in the Northern Hemisphere, increased solute content has been reported in rock-glacier outflows from May to October (Krainer and Mostler, 2002; Krainer et al., 2007), with geochemically-

enriched icemelt that progressively becomes predominant in rock-glacier outflows through the summer and fall seasons, after winter snowpack depletion (Williams et al., 2006).

The large area of mineral surfaces in contact with ice and undergoing chemical weathering in rock glaciers (Ilyashuk et al., 2014, 2017) is hypothesised to enhance the production of concentrated solutes in water (Williams et al., 2006; Fegel et al., 2016). Different hypotheses have been formulated to explain how weather and climate drive the export of solute-rich water from rock glaciers. Thies et al. (2007) proposed that atmospheric warming enhances solute export via ice melt at depth. Williams et al. (2006) suggested that a long-lasting snow cover reduces solute export by delaying subsurface ice melt, which is expected to release solutes, and that solute-rich water is diluted with snowmelt. Similarly, periods of summer rainfall were found to correspond with lower solute contents (Krainer et al., 2007), likely due to the low solute concentration in rain. By contrast, Thies et al. (2007) assumed rainfall to contribute to the export of solutes due to an intensification of water percolation through rock glaciers.

Generally, high-elevation impounded surface waters are considered key freshwater reference sites due to minimal direct human influence and because of their rapid hydrological, physical, chemical, and biological responses to climate-related changes (e.g., Catalan et al., 2006; Adrian et al., 2009; Tolotti et al., 2009; Salerno et al., 2014, 2016). A better understanding of the meteorological drivers responsible for solute export is therefore important for interpreting records of pond water quality and for anticipating and monitoring future changes. In this study, a pond adjacent to an active rock glacier located in the NW Italian Alps is used as a case study. At weekly temporal resolution of observations, a pond has the advantage of integrating signals, which in a stream might otherwise vary too quickly to be sampled adequately (Guzzella et al., 2016; Salerno et al., 2016).

Some previous studies of the chemical characteristics of rock-glacier outflows (Williams et al., 2006; Thies et al., 2013) and lakes (Thies et al., 2007; Ilyashuk et al., 2014, 2017) exist. Their

ability to reveal the response of these systems to meteorological drivers, however, is limited. This is because of low temporal resolution and only partial observation of the relevant meteorological, hydrologic, and chemical variables. Aiming to fill this gap, this study investigates how meteorological variables affect the export of solutes from a rock glacier into an adjacent pond.

In this study, a rock-glacier pond was monitored weekly, while the pond surface was without ice cover (ice-free season), during 2014 and 2015. The link between meteorological variables and hydrochemical characteristics was analysed by comparing air temperature, snowmelt and rainfall with the hydrochemical response of the pond as revealed by water temperature as a proxy of rock-glacier discharge, stable water isotopes, major ions and selected trace elements. Causal relationships between meteorological variables and pond response were investigated by analysing the differences in measured variables among three sampling points in the pond, considered representative of specific water sources.

2. Materials and Methods

2.1 Study area

The Col d'Olen Rock Glacier Pond (45°52'8.22''N, 7°51'46.98''E) is located in the North-Western Italian Alps (Fig. 1a) along the Valle d'Aosta and Piemonte regions border, at an elevation of 2722 m a.s.l.. The catchment area, determined by using a Digital Terrain Model (DTM, cell size: 2 m x 2 m, produced by Regione Autonoma Valle d'Aosta), is approximately 206,000 m^2 (Fig. 1b). The research site is a node of the Long-Term Ecological Research (LTER) network in Italy (http://www.lteritalia.it).

Geologically, from North to South, the Col d'Olen area is structurally composed by: i) the Monte Rosa nappe (micaschists and paragneisses with eclogite maphic rocks and aplitic tabular bodies); ii) the complex Ophiolitic Piedmont Zone, with the "Zermatt-Saas" unit (ophiolitic breccias, quartzite and manganese micaschists, phyllitic schists, and calcschists) and the "Combin Zone" unit

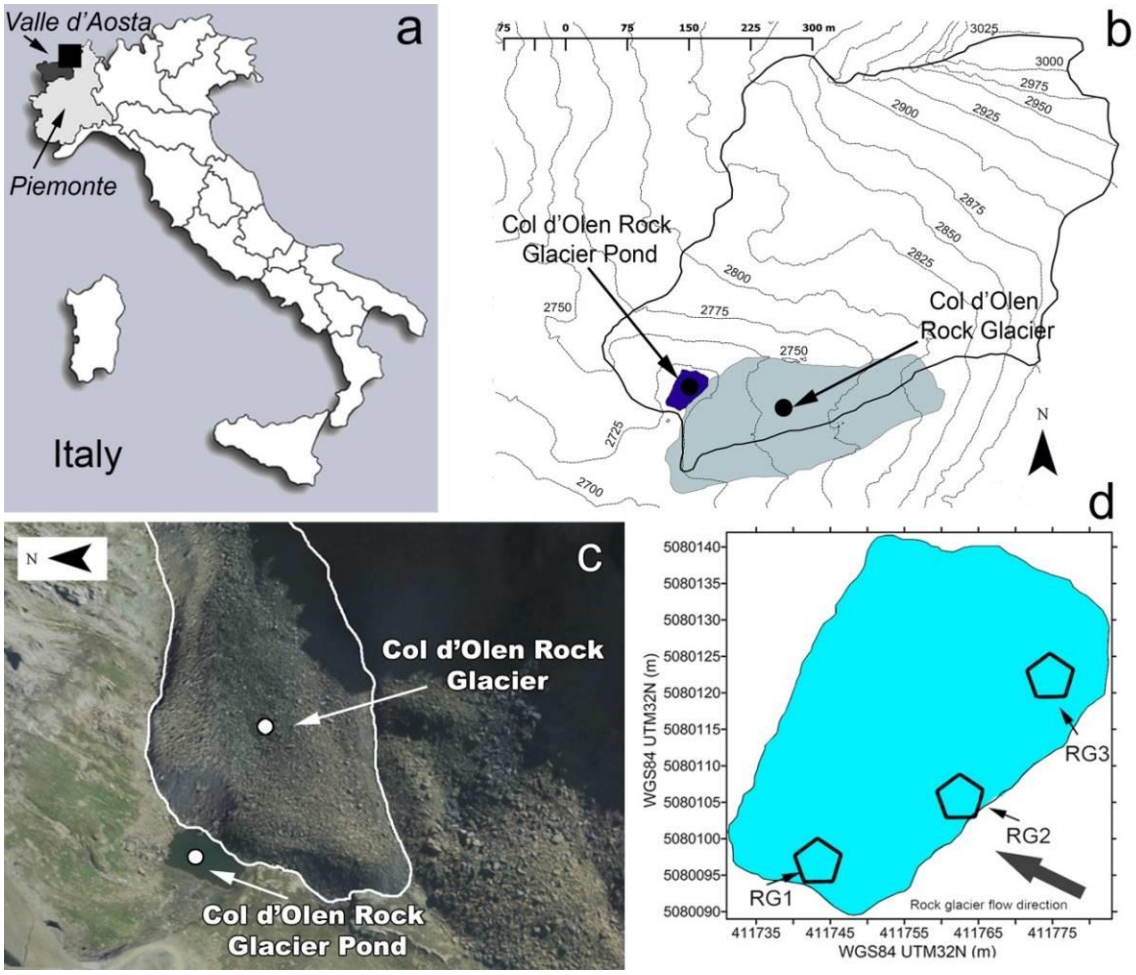

Figure 1 - (a) Location of the study area in Italy. (b) Elevation map of the study area showing the extent of the catchment as delineated from the DTM, the Col d'Olen Rock Glacier and the Col d'Olen Rock Glacier Pond. (c) Three-dimensional view of the Col d'Olen Rock Glacier and the Col d'Olen Rock Glacier Pond (GeoViewer3D Arpa Piemonte, source: http://webgis.arpa.piemonte.it/geoportale). (d) Water temperature sensor locations and water sampling sites in the pond.

(serpentinites and prasinites); and iii) the Sesia Lanzo Zone (gneisses of polimetamorphic origin) (Handy et al., 2010; Gasco et al., 2011; Steck al., 2015).

A high-elevation automatic weather station (AWS) is operated at 800 m distance from the pond (Alpini Corps - Meteomont Service, Italian Army), the Col d'Olen station (2900 m a.s.l.). For the time span 2008–2015, the station recorded a mean liquid precipitation during the ice-free season of 400 mm and a mean annual air temperature of -2.6 °C. The snowpack generally developed by late

October to early November. The snowpack usually becomes isothermal in late May to early June and melt out occurs in July.

The Col d'Olen Rock Glacier ("Corno Rosso 2 Rock Glacier" in the Aosta Valley rock glacier cadastre, http://www.geonavsct.partout.it) typology is a bouldery talus-tongue shaped (cf., Haeberli et al., 2006) (morphometric characteristics are listed in Table 1). The rock glacier is covered by boulders varying from tens of centimetres to several metres in size. Fine-grained sediments surface at the terminus and at the lateral scarps. Serpentinites constitute the main lithology of the fine-grained body, while calcschists and serpentinites are present as clasts and boulders on the surface. The rock glacier seems to be active based on limited lichen growth, sparse vegetation, microform evidence of recent movements in the steep frontal slopes, in addition to fresh and unstable boulders on the surface (Barsch, 1996; Millar and Westfall, 2008). The rock glacier is classified as intact according to the Aosta Valley rock-glacier cadastre. It has a main flow direction from NE to SW, toward a small valley depression where the pond is located (Fig. 1c) and no surficial springs or streams are visible. The contributing area of the rock glacier is 21,800 m^2, this is about 11 % of the pond catchment. Given the possibility for sub-surface flow, the actual contribution area, however, could differ.

The pond has an elongated shape and is situated in front of the rock glacier, on the orographically right, marginal side of the tongue (Fig. 1c and 1d, Tab. 1). Its shoreline is surrounded by the rock glacier from NE to SE, with the front dipping into the pond, from N to SW by slopes with weathering deposits (scree accumulations and pedogenised fine-grained deposits often associated with alpine meadows) and a small rockfall deposit primarily composed of amphibolites, and it is partially bordered on the south by bare bedrock outcrop (calcschists). The pond has no persistent surficial inflows. Only a tiny ephemeral snowmelt stream that usually disappears during the ice-free season (July–August) is present; the stream had dried-out before the start of the investigated ice-free seasons 2014 (25 August to 9 October) and 2015 (9 July to 12

Rock-glacier morphometric characteristics	
Minimum elevation of the front	2706 m a.s.l.
Rooting zone elevation	2816 m a.s.l.
Maximum length	340 m
Maximum width	160 m
Area	37,500 m^2
Maximum height of the front	25 m
Maximum marginal slope	46°
Mean surface slope angle	18°
Pond morphometric characteristics	
Maximum length	60 m
Maximum width	40 m
Perimeter	160 m
Area	1,600 m^2
Maximum depth	3 m

Table 1 - Rock-glacier and pond morphometric characteristics.

October). There are no surficial outflows from the pond and it is thermally mixed during the ice-free season (Colombo et al., 2018b). The pond surface is usually ice-free from mid-July until mid-October. During the two years investigated, the pond surface became ice-free on 25 and 4 July, respectively. In 2014, the sampling season started only on 25 August, one month later than the actual beginning of the ice-free season, because the location of the rock glacier inflow in the pond was only then detected (Colombo et at., 2018b). Based on this experience, the sampling season in the following year could start on 9 July, just a few days after the pond became ice-free.

2.2 Snow cover duration estimation

Snowpack duration in the catchment and on the rock glacier was estimated using three approaches with different spatial and temporal resolutions in order to adequately assess the presence/absence of snow in the catchment and among the boulders of the rock glacier. (i) Hourly data on snow thickness were obtained from the Col d'Olen AWS to monitor local snowpack melt progression. Data were aggregated to daily values and no data gaps were present in the series. (ii)

Landsat 8 (spatial resolution: 30 m, geolocation uncertainty: 3-6 m, Storey et al., 2014) imagery was analysed for the ice-free seasons 2014 and 2015. This provided a coarse resolution estimate of snowpack persistence in the catchment on a weekly to two-weekly basis (further details in Supporting Information (SI), Materials and Methods SI1). (iii) To analyse long-lasting snow among the coarse blocks at the rock-glacier surface, a network of miniature temperature sensors was established to monitor snowmelt based on ground surface temperature (GST) (e.g., Gadek and Leszkiewicz, 2010; Staub and Delaloye, 2016). The melt-out date of snow (when the last snow disappears at a location) was calculated based on the methodology proposed by Schmid et al. (2012). GSTs were measured using miniature temperature loggers Maxim iButton® DS1922L (accuracy ±0.5 °C, resolution 0.0625 °C), programmed to record every three hours from 1 August 2014 to 12 October 2015. 34 loggers were distributed on an equally-spaced grid (26 m x 26 m) in the area of the rock glacier contributing to the pond catchment, buried approximately 10 cm into the ground or placed between and underneath boulders. 32 loggers were retrieved (SI, Fig. SI1) and the three-hourly data were aggregated to daily values. No data gaps were present in the series.

2.3 Meteorological and hydrological measurements

Air temperature was measured at the Col d'Olen AWS. Rain data were obtained from the Gressoney-La-Trinité - Lago Gabiet AWS (managed by Arpa Valle d'Aosta, 2379 m a.s.l., located at 2.5 km distance from the pond) since the rain gauge data from the Col d'Olen AWS had numerous gaps in the ice-free season 2015. Hourly data were aggregated to daily values; no data gaps were present in the series investigated.

To detect the rock-glacier discharge in the pond, Colombo et al. (2018b) integrated waterborne geophysical techniques and a heat-tracer approach based on water temperature difference at three measurement sites in the pond (Fig. 1d). The temperature of sub-surface rock-glacier outflow was estimated at -0.5 °C, 0 °C and +0.5 °C, and assumed constant over time (Krainer et al., 2007; Millar

et al., 2013; Geiger et al., 2014). Lacking persistent surficial pond inflows or outflows, that is a common deficiency at all high-elevated water bodies, the applied methodology allowed to obtain temporal variations in the rate of rock-glacier discharge (Qrock) on total discharge (Qtot) reaching the RG3 sensor (Fig. 1d), providing qualitative information on temporal patterns, although not quantifying the rock-glacier discharge in absolute terms.

2.4 Chemical analyses

Water sampling in the pond was carried out at the same three locations in the pond where water temperature measurements were performed (Fig. 1d), using a telescopic sampling beam. A 300 cm-deep snow profile was sampled before the melting season near the Col d'Olen station in April 2015, and 6 snow samples were collected at 50 cm-intervals for isotopic analyses. A rain collector was installed on the southern part of the pond and sampled for isotopic analyses when precipitation occurred (13 observations).

For every sampling date and at each sampling point, two samples were collected in new 50-ml polyethylene tubes for solute analyses (SI, Materials and Methods SI1). pH was measured using a WTW - InoLab 7110 pH-meter, equipped with Hamilton GelGlass electrode. EC was measured using a Crison - Micro CM 2201 (Colombo et al., 2018b). The concentration of major anions (Cl^-, NO_2^-, NO_3^-, PO_4^{3-}, SO_4^{2-}) was determined with a Dionex DX-500 (Dionex Corp., California), 2 mm system, equipped with an auto-sampler AS50, AS9 analytical column, and AG9 pre-column. The eluent was 9 mM sodium carbonate pumped at a flow rate of 0.25 ml min^{-1}. Major cations (Ca^{2+}, Mg^{2+}, K^+, Na^+) were determined by F-AAS using a Perkin Elmer AAnalyst 400 (Perkin-Elmer Inc., Waltham, Massachusetts). Potential toxic trace elements (Ni, Mn, Co) from the weathering of serpentinites (e.g., Brooks, 1987; Schreier et al., 1987) and generally reported to be highly concentrated in rock glacier outflows (Thies et al., 2013) and lakes (Thies et al., 2007; Ilyashuk et al., 2014) were analysed. These elements were determined using a Thermo Finnigan Element 2

Inductively Coupled Plasma-Mass Spectrometer, able to work at low, medium and high resolution. The quality of chemical analyses was determined by including method blanks and repeated measurements of certified samples. Analytical precision for major anions was <10 %, and for major cations and for trace elements was <5 %. Finally, to verify the possible contribution of soil matrix to trace-element dynamics in the pond, correlations with soil-related contributions, such as organic C, were checked. Dissolved organic carbon (DOC) was determined with a total organic carbon (TOC) analyzer (Elementar, Vario TOC, Hanau, Germany). Analytical precision for DOC was <2 %.

Samples for stable water isotopic analyses ($\delta^{18}O$ and $\delta^{2}H$) were collected using new vials with airtight caps. To determine isotope concentrations an Isotopic Liquid Water Analyzer used a time based, optical absorption spectroscopy of the target gasses (Picarro L2130-i). Analyses for $\delta^{18}O$ and $\delta^{2}H$ were performed at the INSTAAR (Institute of Arctic and Alpine Research) Kiowa Environmental Chemistry Laboratory of the University of Colorado at Boulder (USA). Isotopic compositions are expressed as a δ (per mil) ratio of the sample to the Vienna Standard Mean Ocean Water (VSMOW), where δ is the ratio of $^{18}O/^{16}O$ or $^{2}H/^{1}H$. Analytical precision was 0.05 ‰ for both $\delta^{18}O$ and $\delta^{2}H$. Deuterium excess (d_{excess}) (Dansgaard, 1964) was also analysed to provide insight into the potential importance of melt-freeze cycles characterising the outflow from the rock glacier (Steig et al., 1998; Williams et al., 2006). d_{excess} was computed for each sample following the protocol developed by Johnsen and White (1989) based on the equation for the Global Meteorological Water Line (GMWL, Craig, 1961).

2.5 Statistical analyses

Statistical analyses were performed using the programming language R (R Development Core Team, 2011). Principal Component Analysis (PCA), a multivariate ordination technique, was conducted to interpret the major patterns of variation in the data. Data were centred and

standardised to mean zero and unit variance so that all variables were comparable. The degree of correlation among data was verified through the correlation coefficient (r) (e.g., Venables and Ripley, 2002).

3. Results

3.1 Snow cover duration

The two ice-free seasons 2014 and 2015 had different snow-depletion periods. Col d'Olen AWS data showed that the snowpack was absent from the beginning of August in 2014 (Fig. 2a) and from the beginning of July in 2015 (Fig. 2b). Landsat data showed that in 2014, the last snow in the catchment was present on 19 July (catchment 1 % snow covered) (Fig. 2a). In 2015, no snow was found at the beginning of the ice-free season (Fig. 2b). The spatially distributed temperature logging showed that, in 2014, no snow was present on the rock-glacier surface from the date of first water sampling (25 August). During the ice-free season 2015, melt-out date of snow ranged from 6 June to 7 July 2015 (SI, Fig. SI2), with snowpack depletion occurring before the start of the ice-free season on 9 July.

3.2 Meteorological conditions

Similar to snow cover duration, air temperature during the ice-free seasons 2014 and 2015 was different. In July–August 2014 the mean air temperature was lower (mean: +3.4 °C) (Fig. 2c) than the air temperature in the same period in 2015 (mean: +6.4 °C) (Fig. 2d). Conversely, the air temperature in September and during the first ten days of October 2014 was higher (mean: +1.8 °C) (Fig. 2c) than the air temperature in the same time-span in 2015 (mean: -0.2 °C) (Fig. 2d).

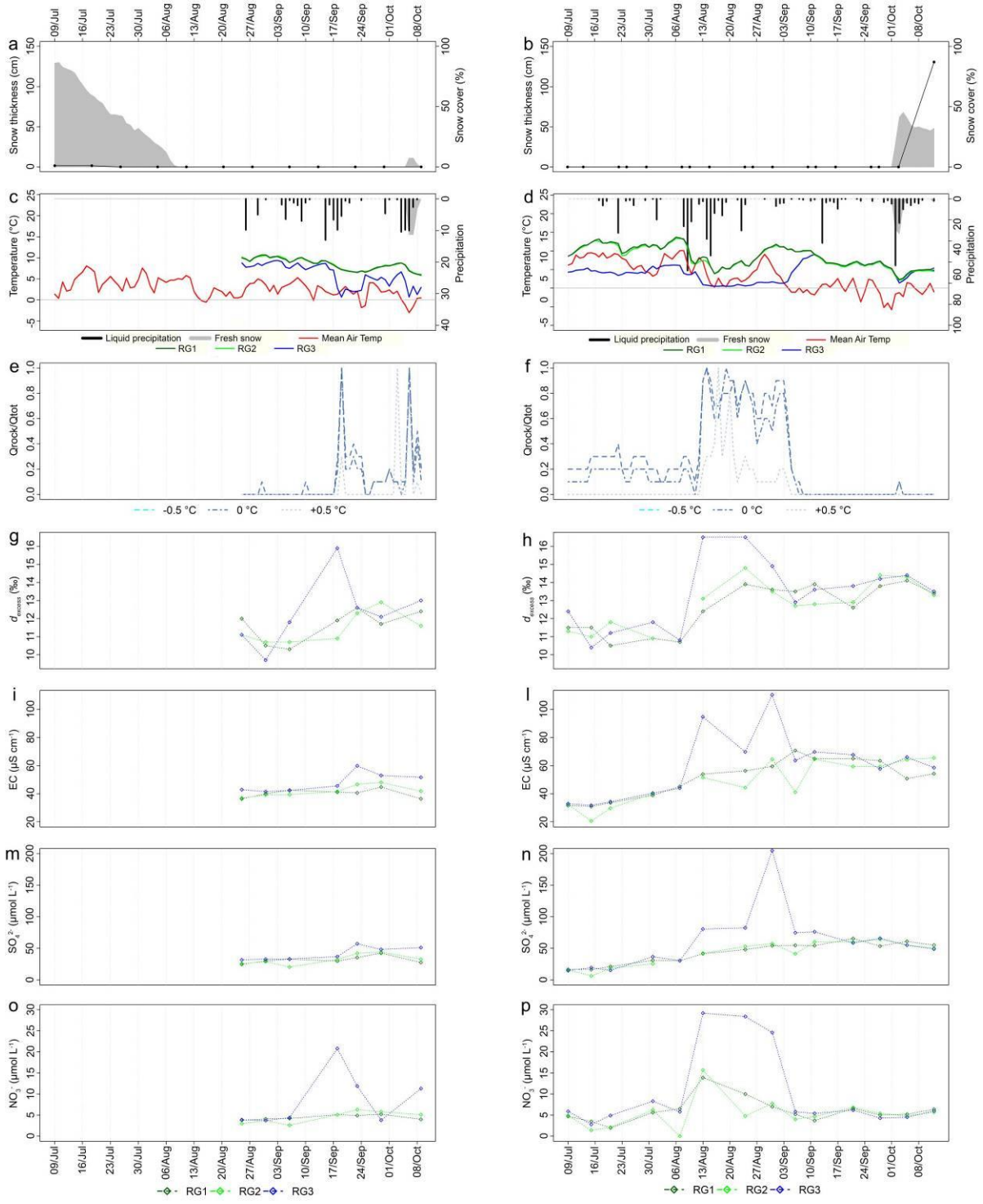

Figure 2 - Data series for the ice-free seasons 2014 (left) and 2015 (right). (a-b) Snow thickness (cm) (grey polygons) and percentage of catchment covered by snow (%) from Landsat data (black line, dots represent analysed images, those with cloud cover were excluded). (c-d) Mean daily liquid precipitation (mm), fresh snow (cm), air temperature (°C), and water temperature (°C) at RG1, RG2 and RG3 (please note that c and d have different secondary y-axes). (e-f) Relative rock-glacier

contribution expressed as ratio Qrock/Qtot (details in the main text) in the pond with the temperature of the cold-water from the rock glacier estimated at -0.5 °C, 0 °C and +0.5 °C. (g-h) d_{excess} values (‰) at RG1, RG2 and RG3. (i-l) EC values (µS cm^{-1}). (m-n) SO_4^{2-} concentration (µmol L^{-1}). (o-p) NO_3^- concentration (µmol L^{-1}) (modified from Colombo et al., 2018b).

Precipitation was less abundant during the sampling season 2014 (no precipitation event exceeded 20 mm, Fig. 2c) than in 2015 (six precipitation events exceeded 20 mm, Fig. 2d). Liquid precipitation events were mainly concentrated in September and early October 2014 (Fig. 2c), and in August 2015 (Fig. 2d).

3.3 Rock-glacier discharge

Daily water temperature during the ice-free seasons 2014 and 2015 at RG3 (mean: +4.7 °C) was lower than water temperature at RG1 (mean: +8.5 °C) and RG2 (mean: +8.4 °C) (Fig. 2c and 2d). The difference between RG2, which showed an almost identical pattern to RG1 both in 2014 and 2015 (Fig. 2c and 2d), and RG3 was used to infer the relative discharge coming from the rock glacier on a daily basis (Colombo et al., 2018b). The results showed that in the ice-free season 2014, two main peaks of rock-glacier discharge were estimated from mid-September, just before the end of the ice-free season, on 19 September and 6 October (Fig. 2e). During the ice-free season 2015, a long and almost continuous high-discharge period was detected from 14 August to 3 September (Fig. 2f).

In both years, high discharge was observed before air temperature became negative or close to 0 °C. This was particularly evident in 2015 before mid-September, when average daily air temperature became negative (Fig. 2d), and water temperature recorded by all sensors (RG1, RG2, and RG3) became equal, i.e., a clear signal of the rock-glacier discharge interruption (Fig. 2d). Hereafter, the period of higher discharge observed during both sampling years (from 17 September

to 9 October 2014, and from 11 August to 11 September 2015 - until the RG3 water temperature converged with the water temperature at RG1,2) will be named high-discharge (HD) period and the remaining period as low-discharge (LD) period. The delay time between main precipitation events and discharge peaks was found to range from 6 hours to 3 days. It is important to note that no measurements were performed during periods in which rock-glacier discharge is usually reported to be the highest due to snowpack melting (May–June) (e.g., Krainer and Mostler, 2002; Krainer et al., 2007) because the ice cover on the pond surface is, on average, present until mid-July.

3.4 Water isotopes

Isotopic values of water samples showed the main differences between RG3 and RG1,2 during the HD period (Tab. 2). For instance, average RG3 and RG1 d_{excess} difference during the HD period was +1.56 ‰, while the difference during the LD period was +0.23 ‰. Although less evident than d_{excess}, $\delta^{18}O$ and $\delta^{2}H$ became more enriched at RG3 than at RG1,2 during the same period (Tab. 2). As a benchmark of the system, snow and rain were also sampled. Snow was characterised by the lowest $\delta^{18}O$ (mean: -18.9 ‰), $\delta^{2}H$ (mean: -139.26 ‰), and d_{excess} (mean: 11.7 ‰) values. Contrarily, rain showed the highest $\delta^{18}O$ (mean: -10 ‰), $\delta^{2}H$ (mean: - 64 ‰), and d_{excess} (mean: 15.9 ‰) values, with no temporal pattern in the series (not shown).

	$\delta^{18}O$ (‰)			$\delta^{2}H$ (‰)			d_{excess} (‰)		
	RG1	**RG2**	**RG3**	**RG1**	**RG2**	**RG3**	**RG1**	**RG2**	**RG3**
LD (13 observations)	-12.74 (0.96)	-12.74 (1.01)	-12.75 (0.98)	-89.93 (8.80)	-89.82 (9.25)	-89.79 (9.04)	11.97 (1.41)	12.08 (1.38)	12.20 (1.55)
HD (8 observations)	-12.02 (0.82)	-12.01 (0.77)	-11.83 (0.62)	-83.40 (6.92)	-83.38 (6.87)	-80.34 (6.31)	12.75 (0.83)	12.72 (1.19)	14.31 (1.84)

Table 2 - Isotopic measurements for the sampling sites during low-discharge (LD) and high-discharge (HD) periods in 2014 and 2015. Mean value and standard deviation (in brackets) are reported.

3.5 Water chemical composition

EC showed higher values at RG3 than at RG1,2 during the HD period (Tab. 3) in 2014 (Fig. 2i) and 2015 (Fig. 2l). For major anions, the main differences among the sampling points in the pond were found for SO_4^{2-} (Fig. 2m and 2n) and NO_3^- (Fig. 2o and 2p), with higher concentrations at RG3 during the HD period, similar to EC (Tab. 3), as expected. Concentration increases of the major cations Mg^{2+} (Fig. 3a and 3b) and Ca^{2+} (Fig. 3c and 3d) were measured at RG3 in the same period (Tab. 3). Na^+ and K^+ concentrations were lower compared with those of Mg^{2+} and Ca^{2+} and did not show specific temporal patterns (not shown) although during the HD period they were slightly more diluted at RG3 than at RG1,2 (Tab. 3). The trace elements Ni, Mn and Co were more concentrated at RG3 than at RG1,2 (Tab. 3) during the HD period in 2014 (Fig. 3e, 3g, and 3i), and from mid-July to mid-September 2015, with the greatest differences measured during the HD period in 2015 (Fig. 3f, 3h, and 3l). An initial peak in trace-element concentrations was also found at the beginning of the ice-free season 2015 (Fig. 2f, 2h, and 2l). For each sampling point, weak negative correlation between DOC and trace elements occurred at RG1 with DOC and Ni ($r=-0.44$; $p<0.1$) and DOC and Co ($r=-0.38$; $p<0.1$), and at RG2 between DOC and Ni ($r=-0.47$; $p<0.05$) and DOC and Co ($r=-0.64$; $p<0.01$). No correlation occurred at RG3 (SI, Tab. SI1).

	EC (µS cm^{-1})			pH			Cl$^-$ (µmol L^{-1})		
	RG1	**RG2**	**RG3**	**RG1**	**RG2**	**RG3**	**RG1**	**RG2**	**RG3**
LD (13 observations)	46.0 (12.6)	46.0 (15.7)	48.5 (13.7)	7.5 (0.2)	7.4 (0.2)	7.4 (0.2)	2.5 (2.0)	2.2 (1.5)	2.4 (1.4)
HD (8 observations)	50.5 (11.7)	47.5 (7.8)	68.6 (22.7)	7.5 (0.1)	7.6 (0.3)	7.5 (0.1)	2.4 (1.9)	1.5 (0.4)	3.0 (0.8)

	SO_4^{2-} (µmol L^{-1})			NO_3^- (µmol L^{-1})			Mg^{2+} (µmol L^{-1})		
	RG1	**RG2**	**RG3**	**RG1**	**RG2**	**RG3**	**RG1**	**RG2**	**RG3**
LD (13 observations)	38.0 (17.5)	36.0 (20.5)	40.0 (19.5)	4.7 (1.4)	3.9 (2.0)	5.1 (1.4)	98.9 (27.0)	89.9 (35.8)	103.6 (33.4)
HD (8 observations)	41.8 (10.3)	43.2 (8.8)	79.5 (53.2)	6.9 (3.4)	6.8 (3.8)	17.0 (10.1)	111.8 (21.0)	110.0 (14.9)	165.4 (23.1)

	Ca^{2+} (µmol L^{-1})			K^+ (µmol L^{-1})			Na^+ (µmol L^{-1})		
	RG1	**RG2**	**RG3**	**RG1**	**RG2**	**RG3**	**RG1**	**RG2**	**RG3**
LD (13 observations)	101.4 (24.3)	100.0 (31.9)	102.1 (25.6)	10.7 (3.8)	9.9 (4.1)	10.6 (4.4)	5.9 (2.0)	5.7 (3.0)	5.3 (1.4)
HD (8 observations)	121.6 (11.4)	124.7 (14.8)	143.7 (25.4)	10.9 (4.5)	9.6 (3.1)	6.9 (3.4)	4.7 (1.1)	5.7 (2.1)	4.6 (1.9)

	Ni (nmol L^{-1})			Mn (nmol L^{-1})			Co (nmol L^{-1})		
	RG1	**RG2**	**RG3**	**RG1**	**RG2**	**RG3**	**RG1**	**RG2**	**RG3**
LD (12 observations)	197.2 (78.0)	217.6 (79.3)	257.3 (135.6)	24.1 (45.4)	24.3 (48.7)	39.2 (60.2)	0.9 (0.6)	0.8 (0.6)	1.1 (0.7)
HD (8 observations)	192.2 (53.9)	213.0 (43.4)	509.1 (192.8)	22.5 (18.7)	31.2 (26.3)	94.5 (66.9)	1.1 (0.6)	1.3 (0.7)	2.3 (0.9)

Table 3 - Solute concentrations in the water sampling sites during low-discharge (LD) and high-discharge (HD) periods in 2014 and 2015. Mean value and standard deviation (in brackets) are reported. NO_2^- and PO_4^{3-} were below the detection limits.

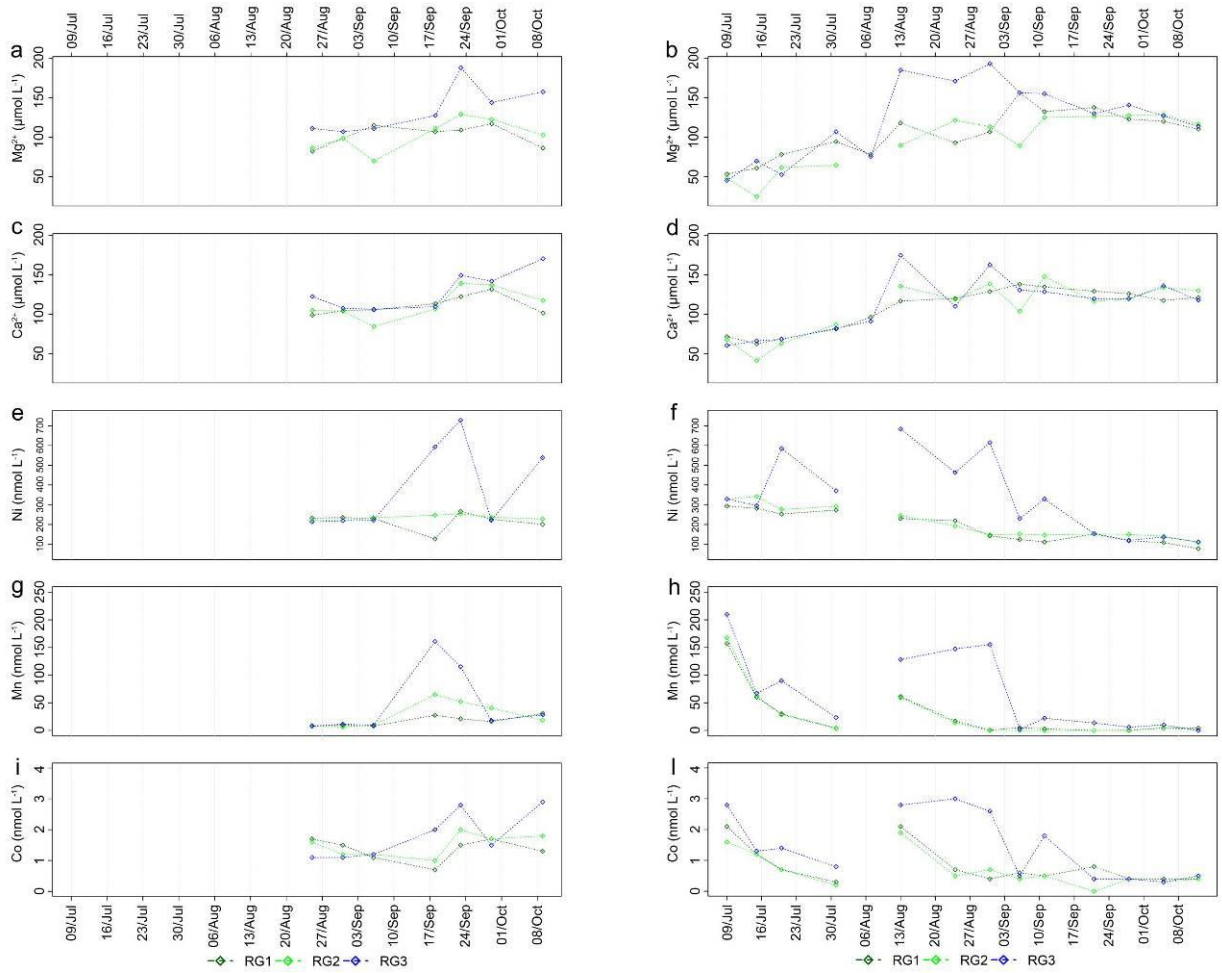

Figure 3 - Data series for the ice-free seasons 2014 (left) and 2015 (right). (a-b) Mg^{2+} concentration at RG1, RG2 and RG3 (µmol L^{-1}). (c-d) Ca^{2+} concentration (µmol L^{-1}). (e-f) Ni concentration (nmol L^{-1}). (g-h) Mn concentration (nmol L^{-1}). (i-l) Co concentration (nmol L^{-1}).

4. Discussion

The integrated analyses of water temperatures, estimated relative rock-glacier discharge, stable water isotopes and solute content revealed systematic patterns. In both ice-free seasons, RG1 and RG2 generally showed similar patterns, while higher chemical concentrations were measured at RG3 (Fig. 2 and 3). There, increases of inferred rock-glacier discharge (Fig. 2e and 2f) were found to be temporally associated with isotopically-enriched waters, particularly evident for d_{excess} (Fig. 2g and 2h).

4.1 Rock-glacier hydrological contributions

HD periods in 2014 (Fig. 2e) and 2015 (Fig. 2f) occurred after the melting of the snowpack (Fig. 2a, 2b, and SI, Fig. SI2) thus, the contribution of snowmelt on rock-glacier discharge can be excluded. Higher air temperatures in July–August 2015 (mean: +6.4 °C) in comparison to July–August 2014 (mean: +3.4 °C) (Fig. 2c and 2d) enhanced the melting of the snowpack, resulting in its complete depletion in the catchment and on the rock glacier one month earlier in 2015 than in 2014 (Fig. 2a and 2b). A long-lasting winter snowpack in 2014 probably contributed to delaying the onset of active-layer thawing (cf., Hanson and Hoelzle, 2004). Conversely, higher air temperatures in September and during the first ten days of October 2014 (mean: +1.8 °C) than during the same time in 2015 (mean: -0.2 °C) (Fig. 2b and 2c) contributed to the extension of the thawing season until October 2014 (Fig. 2e), while no evidence of rock-glacier discharge was found in the pond from mid-September 2015 (Fig. 2f). The air temperature difference between the two years investigated is reflected in the dynamics of the distributed GST measurements on the rock glacier. Indeed, in the first part (until the end of August) of the ice-free season 2014 mean GSTs were lower (+6.1 °C) than in 2015 (+8.9 °C). Conversely, during the second part (in September and during the first ten days of October) of the ice-free season 2014 mean GSTs were warmer (+4.4 °C) than in 2015 (+2.3 °C), with GSTs generally close to 0 °C or negative after mid-September 2015 (not shown). Since the beginning of September 2015, mean air temperatures were negative or close to 0 °C values for several days (Fig. 2d). During this period, low water temperature at RG3 progressively increased until convergence with temperatures at RG1,2 (Fig. 2d), when the HD period stopped (Fig. 2f).

HD periods from the rock glacier were found to be associated with liquid precipitation during the ice-free seasons 2014 (Fig. 2c and 2e) and 2015 (Fig. 2d and 2f). In general, rain events increased the export of cold water from the rock glacier at RG3 and this is assumed to be due to the contact of water with melting ice in the subsurface (Krainer and Mostler, 2002; Berger et al., 2004; Krainer et

al., 2012; Millar et al., 2013). This was evident from mid-September to the end of the ice-free season 2014 (Fig. 2c), and from mid-August to mid-September 2015 (Fig. 2d). Previously, intense summer rainfall has been reported to cause peaks in discharge from rock glaciers while water temperature usually remains stable around the freezing point (Krainer and Mostler, 2002; Berger et al., 2004; Krainer et al., 2007; Geiger et al., 2014). Our observations likely reflect the same pattern where higher cold discharge contributes to the temperature signal observed at RG3. Moreover, water infiltration can lead to a rapid warming of the ground at depth through thermal advection and release of latent heat (Rist and Phillips, 2005), in turn leading to higher unfrozen water content, especially if temperatures are close to 0 °C (Anderson et al., 1973; Arenson et al., 2002).

The delay between precipitation events and discharge peaks ranged from 6 hours to 3 days. In the latter case, snow melting after each precipitation event was the main driver of discharge delaying. Generally, delay time ranged from 6 hours to 1 day after rainfall events. Rainfall periods have been reported to cause great variations in groundwater circulation in rock glaciers and even dry springs can reactivate after heavy and/or repeated rainfall events (Kummert et al., 2017). Moreover, highly variable residence times, ranging from few hours to several days, of water in rock-glacier bodies have been reported in the scientific literature and are likely based on internal characteristics such as hydraulic connectivity, active-layer thickness and sedimentological composition, or the amount and characteristics of internal ice (Tenthorey, 1992, 1993; Harris et al., 1994; Krainer and Mostler, 2002; Berger et al., 2004; Buchli et al., 2013). The residence time in the investigated rock glacier is likely to indicate that the flow path in the landform is heterogeneous and the hydraulic connection is poor (Tenthorey, 1992, 1993; Harris et al., 1994). Moreover, percolating water might flow through fine-grained unsaturated terrain at larger depths due to a great active layer thickness, resulting in small flow velocity in the rock-glacier interior (cf., Buchli et al., 2013). Flowing water was neither seen nor heard between the coarse debris, and this has been previously attributed to the presence of meltwater channels eroded into the frozen rock-glacier body (Krainer

and Mostler, 2002; Berger et al., 2004). Keeping in mind that the flow of the rock-glacier water into the pond is localised and sub-surficial, it is possible that part of the flow path is in fine-grain sediments and in bedrock fractures (Colombo et al., 2018b), thus further increasing the residence time of water in the system. The observed residence times are similar to the delay detected between events of strong precipitation and peaks in rock-glacier movement (Wirz et al., 2016).

4.2 Isotopic signature of the pond water

During the HD period, d_{excess} increased, reaching maximum values at RG3 both in 2014 and 2015 (Fig. 2g and 2h). In this period, d_{excess} values at RG3 (max.: 16.5 ‰, mean: 14.3 ‰) were closer to those of rain (max.: +19.5 ‰, mean: +15.9 ‰) than of snow (max.: +13.3 ‰, mean: +11.7 ‰). A mean d_{excess} value for snow of about +11 ‰ was reported by Williams et al. (2006) in their study on the Green Lake 5 rock glacier, similar to the base value for the ice core of the Galena rock glacier (Steig et al., 1998). Williams et al. (2006) found increasing d_{excess} values in the rock-glacier outflow during the summer season, with a maximum value of +17.5 ‰ in the fall. An enrichment of +6 ‰ compared to snow is similar to the values for sections of the ice core from the Galena rock glacier that had undergone multiple melt-freeze cycles (Steig et al., 1998). In our study, a smaller enrichment was found at RG3, but it is worth noting that the mixing with more depleted pond water is likely to smooth the enriched isotopic signal coming from the rock-glacier into the pond. Williams et al. (2006) attributed the d_{excess} enrichment in the rock-glacier outflow to icemelt subject to multiple melt-freeze cycles. The authors also reported that some combination of isotopically-enriched rainwater and icemelt could have potentially provided the same isotopic values in the outflow of the rock glacier. However, in that case, the effect of rain was considered minimal due to its small contribution to annual precipitation. In our case, giving the mixed origin (i.e., rain, icemelt, groundwater) of the water source at RG3 (further mixed with pond water) and the fact that it is not easy to discriminate among these different components, the contribution of ice melt, here

considered as originating from a mixture of ice and debris, to the hydrological budget cannot be well constrained (cf., Krainer et al., 2007). However, the effect of rainwater alone can be excluded because strong increases in d_{excess} at RG3 were only found during the HD period and did not occur during other rainfall events in the ice-free seasons (Fig. 2c and 2d); this is particularly evident during the last month of the ice-free season 2015. Moreover, if this was only an effect of rainwater flowing from the catchment to the pond and directly falling into the pond, one would expect similar behaviours among all sampling points, with no such strong enrichment preferentially affecting RG3. Evaporation could also influence the isotopic trends in the pond (cf., Jonsson et al., 2009), with implications for d_{excess} dynamics (cf., Yuan et al., 2011). However, d_{excess} values were similar at RG1, RG2 and RG3 for several sampling dates, both in 2014 (Fig. 2g) and 2015 (Fig. 2h). Indeed, these values derived from the mixing effect of all hydrological components in/from the pond (also including the evaporation), influencing all the sampling points. Only during the estimated HD periods, d_{excess} values at RG3 deviated substantially from the values measured at RG1,2. Considering the small dimensions of the pond, evaporation should act similarly at all the investigated sampling points. In fact, during LD periods, d_{excess} values were rather similar among the sampling points in the pond. Thus, this might indicate that the cold water at RG3 originated from a combination of isotopically-enriched rainwater and icemelt subject to multiple melt-freeze cycles (Steig et al., 1998; Williams et al., 2006). Although less evident, $\delta^{18}O$ and $\delta^{2}H$ became more enriched at RG3 than at RG1,2 during the HD period (Tab. 2). Isotopic enrichment trends were observed in the outflows of other rock glaciers (Williams et al., 2006; Krainer et al., 2007) and were attributed primarily to the progressive decrease of isotopically-depleted snowmelt and secondarily to higher contribution of isotopically-enriched rain and icemelt plus groundwater.

At the beginning of the ice-free season 2015 (until mid-August), although relative rock-glacier discharge was estimated to be low to moderate (ranging between 0.1 and 0.4, Fig. 2f), RG3 did not show the strong isotopic enrichments as during the HD period. This can be explained with the

presence of cold and rather isotopically-depleted snowmelt coming from the rock glacier, although snow was estimated to be absent in the catchment and on the rock glacier (Fig. 2a, 2b, and SI, Fig. SI2). Thus, it might be possible that, even if investigated at fine-scale with a grid of surficial ground thermal sensors, the potential effects of "hidden" long-lasting snow patches melting among the boulders require an improvement of the measurement setting. Moreover, ice might have accumulated by refreezing of snowmelt after percolating into the active layer (Hinkel et al., 2001; Rist and Phillips, 2005; Juliussen et al., 2008; Woo, 2012) or on top of an ice-rich body inside the rock glacier. This ice might have melted during the warm July-August 2015 period, providing a combination of snowmelt (isotopically-depleted), surficial icemelt (isotopic signature similar to snowmelt), and potential minor internal icemelt (isotopically-enriched) and thus resulting in a rather depleted isotopic signature. This could have led to an inflow of cold and rather isotopically-depleted water from the rock glacier without strong concentration differences among sampling points due to its reduced discharge and because of the presence of isotopically-depleted snowmelt water at the beginning of the ice-free seasons in the pond (cf., Krainer et al., 2007; Jeelani et al., 2010; Penna et al., 2014).

4.3 Export of solutes from the rock glacier

Similar to isotopes, the times of strong differences in solute concentrations between RG3 and RG1,2 corresponded with the HD period. This was shown mainly by EC and SO_4^{2-} trends in 2014 (Fig. 2i and 2m) and 2015 (Fig. 2l and 2n), with this evidence particularly accentuated in 2015. Similar behaviour was found for Mg^{2+} (Fig. 3a and 3b) and Ca^{2+} (Fig. 3c and 3d). Furthermore, trace elements associated with serpentinite weathering (Ni, Mn, Co) strongly increased at RG3 during the HD period, although they were found to be temporally anticipated with respect to major ions. Trace elements also evidenced an initial peak at the beginning of the ice-free season 2015 (Fig. 3).

In the present study, increases in EC and major ions (SO_4^{2-}, Mg^{2+}, Ca^{2+}) were found in late summer and early fall, in agreement with previous studies (Krainer and Mostler, 2002; Berger et al., 2004; Williams et al., 2006; Krainer et al., 2007; Thies et al., 2013). They were, however, also associated with higher rock-glacier discharge after liquid precipitation events. This association, to the best of our knowledge, has been observed here for the first time. Indeed, some previous studies reported dilution of rock-glacier outflow after rainfall due to its low solute content (Krainer and Mostler, 2002; Berger et al., 2004; Krainer et al., 2007). Since increasing EC and major-ion concentrations were found after the winter snowpack had melted and were associated with higher rock-glacier discharge after rainfall, it is likely that this results from the export of geochemically-enriched icemelt (Williams et al., 2006), strong enough to dominate over possible dilution with solute-poor precipitation water. As already observed for isotopes, the effect of rainwater alone can be excluded since different rain events occurred during the investigated ice-free seasons but strong solute increase at RG3 was always associated with HD periods (Fig. 2 and 3). This excludes the possibility of a simple flushing of solutes from micropores during higher flows or other reactions in the rock-glacier fine-grained sediment interior (Clow and Drever, 1996). However, variations of solute concentrations in response to changes in discharge are usually modest (Clow and Drever, 1996), generally evidencing relatively small declines to great discharge increases (Clow and Mast, 2010) through the "chemostatic" behaviour (Godsey et al., 2009). Additionally, rainfall events are usually reported to lower solute concentrations in mountain surface waters, showing strong concentration-flow relationships, especially for weathering-related ions (Froehlich et al., 2008; Goulsbra et al., 2014; Blumstock et al., 2015). Finally, increasing solute concentrations were systematically found at RG3, which is inconsistent with the assumption of the effects of rain flowing from the catchment and/or directly falling into the pond, which should influence all the sampling sites.

In this study, SO_4^{2-} was found to increase at RG3 during the HD period (Fig. 2m, 2n, and Tab. 3). Icemelt from rock glaciers has been assumed to be enriched in SO_4^{2-} (Thies et al., 2007; Thies et al., 2013; Ilyashuk et al., 2014) due to enhanced chemical weathering of freshly exposed mineral surfaces in an environment with high availability of moisture (Williams et al., 2006). In the present study, this includes fine-grain serpentinite detritus and the potential presence of sulphide minerals such as pyrite. Lower sulphate concentrations in RG1,2 suggest that the higher sulphate at RG3 is not derived from fresh mineral surfaces produced by shallow frost weathering (cf., Roy and Hayashi, 2009) but rather derived from the frozen debris-ice mixture in the rock glacier. SO_4^{2-} can also be locally generated by the mineralisation of organic matter in peaty soils (Blodau et al., 2007), but these are absent in the sampling point surroundings. Moreover, Colombo et al. (2018b) collected two surficial lacustrine sediment cores from the deepest area of the pond (approx. 2.5÷3 m water depth) and assessed the presence of organic S compounds (Total S content ranging from 0.4 to 0.6 g kg^{-1}). Sulphur cycling in aquatic sediments involves both reductive and oxidative processes (Jørgensen, 1988, 1990) and might influence sulphate concentrations in the water (Holmer and Storkholm, 2001). However, since the pond is well mixed during the ice-free season (Colombo et al., 2018b), potential sediment-water interactions affect all the sampling points in the pond. SO_4^{2-} concentrations were found to be similar among the sampling points during LD periods, with increases at RG3 only during HD periods, thus excluding a potential localised influence of lacustrine sediments on SO_4^{2-} dynamics at RG3. Also, Mg^{2+} was found to increase at RG3 during the HD period (Fig. 3a, 3b, and Tab. 3); its source can be serpentinites, which are usually enriched in Mg^{2+} (Vithanage et al., 2014; Baumeister et al., 2015), and constitute the fine-grained sediment rock-glacier body. Similarly but less pronounced, Ca^{2+} increased at RG3 concurrent with the HD period (Fig. 3c, 3d, and Tab. 3). This can be explained by the fact that even though serpentinite rocks are depleted in essential nutrients such as Ca^{2+}, K^{+}, and P (Baumeister et al., 2015), the presence of calcschists on the rock-glacier surface might be expected to result in higher

concentrations of Ca^{2+} (Touhari et al., 2014). Thus, icemelt is expected to be primarily enriched in SO_4^{2-} and other weathering products from serpentinites such as Mg^{2+} and, secondarily, of Ca^{2+} from carbonate dissolution deriving from surficial rocks during percolation of snow meltwater and/or rain in the ground (Baltensperger et al., 1990; Haeberli et al., 1999). Flowing of rain on and through the internal sediment-ice matrix during the thawing season is assumed to be the main driver of solute export from the rock glacier, with soluble ions released by thaw and made available for flushing. A similar process has been comprehensively described by Lamhonwah et al. (2017) in a High Arctic catchment on Melville Island, Canada. The authors found rainfall events to act as a flushing mechanism, mobilising solutes from the subsurface (ice-rich layers in the upper permafrost) to surface waters.

Greater differences for EC and major ions between RG3 and RG1,2 were found in 2015 than in 2014 (Fig. 2 and 3). This is consistent with the observation of earlier snow melt-out in 2015 (Fig. 2b) than in 2014 (Fig. 2a), which likely increased subsurface melt and corresponding export of solutes (cf., Williams et al., 2006). However, a very thin snow cover can cool the ground due to reduced thermal insulation (Luetschg et al., 2008) and thus may reduce the summer export of solutes from a rock glacier. Generally, EC and solute content in the Col d'Olen Rock Glacier Pond were comparable to values measured in rock-glacier outflows in catchments composed of metamorphic rocks (Krainer and Mostler, 2001a,b, 2002; Berger et al., 2004; Krainer et al., 2007), but lower than values measured in other rock-glacier outflows (Williams et al., 2006; Thies et al., 2013) and lakes (Thies et al., 2007; Ilyashuk et al., 2014).

Regarding NO_3^-, previous studies in high-mountain regions considered it as a specific marker of microbial activity. For instance, the nitrate in the outflow of talus and blockfields appears to result primarily from microbial activity (Williams et al., 1997; Ley and Schmidt, 2002; Ley et al., 2004) where the microbes are carbon limited and hence move the nitrogen cycle towards net nitrification (Williams et al., 2007). At our site, NO_3^- was found to strongly increase at RG3 during the HD

period both in 2014 (Fig. 2o) and 2015 (Fig. 2p). This is in agreement with other studies in mountain permafrost areas, where increasing nitrate concentration in surface waters was attributed to melting ice in permafrost and rock glaciers (Williams et al. 2007; Baron et al., 2009; Fegel et al., 2016). Microbial communities adapted to extreme environments have been suggested as potential sources of the elevated nitrate in rock-glacier outflows (Williams et al. 2007). Additional research in the Rocky Mountains suggested the observed nitrate increase in surface waters may also be a result of meltwater flushing microbially-active sediments following permafrost degradation (Barnes et al., 2014) and active microbial populations in sediment pockets within talus deposits (Ley et al., 2004). Nitrate leaching is also possible from organic soil horizons during higher flow (Walling and Webb, 1986), but as these are absent on the rock glacier, nitrate increase at RG3 are not attributed to the leaching from the soil. In this study, NO_3^- concentrations in the pond, except during the HD period at RG3, were comparable to those measured in a rock-glacier lake in the Central Eastern European Alps (Ilyashuk et al., 2014) and other high-elevation surface waters (Balestrini et al., 2014; Magnani et al., 2017), but lower than those measured in other rock-glacier outflows in the Colorado Front Range (Williams et al., 2007).

Trace elements associated with serpentinite weathering (Ni, Mn, Co) strongly increased at RG3 during the HD period both in 2014 and 2015 (Fig. 3 and Tab. 3). This pattern is in agreement with previous observations of higher metal concentrations in rock-glacier ponds (Thies et al., 2007) and rock glacier outflows (Thies et al., 2013) in comparison to reference surface waters not influenced by rock glaciers, even though these studies did not investigate intra-seasonal trends. Increasing export of trace elements from permafrost during the late melt season has been also reported in Arctic areas and attributed to a thickening active layer, exposing previously frozen soil to mineral weathering processes (Barker et al., 2014). Soil solution might be responsible for the export of trace elements since it is generally enriched in DOC, which can increase the mobility of metal ions (Rember and Trefry, 2004). In this case, a positive correlation between DOC and the concentration

of trace elements during the HD period would be expected. However, at RG3, no relationship between DOC and trace elements was found (SI, Tab. SI1), further indicating that soil is not involved in ion discharge processes of the rock glacier. Interestingly, increases in trace elements at RG3 were found to be earlier than those of major ions (Fig. 3). This is particularly evident in 2015, when increases in trace elements at RG3 were measured not only during the HD period (mid-August to mid-September), but also in July when the relative discharge of the rock glacier was calculated to range between 0.1 and 0.4 (ratio Qrock/Qtot), especially after a period characterised by some precipitation events (mid-July) (Fig. 2f). Thus, it is possible that these elements are more easily exported from a matrix of sediment and ice derived from ultramafic rocks like serpentinites. Moreover, an initial peak in trace-element concentrations was found at the beginning of the ice-free season 2015 (Fig. 3). One explanation might be the release of trace elements from the melting snowpack before the onset of the ice-free season in the pond, potentially incorporated into snowmelt from upper soil horizons in the catchment (Rember and Trefry, 2004; Bagard et al., 2011). Moreover, the thick ice cover on the pond for eight to nine months during the winter might be accompanied by a decrease in pH caused by CO_2 oversaturation of water (Wögrath and Psenner, 1995). This would prevent the transfer of most trace elements from the water phase to the sediment and cause a desorption from the sediments, resulting in increased concentrations of free metal ions (Salomons, 1995). Mixing of water during the ice-free season would then promote the progressive decrease of trace-element concentrations, as observed in the pond except during the HD period (Fig. 2 and 3). Generally, trace-element concentrations in this study were lower than the ones measured previously in rock-glacier outflows (Thies et al., 2013) and rock-glacier lakes (Ilyashuk et al., 2014) in the Central Eastern Alps, probably due to different local settings. More research is needed to further explain these differences, since considerable uncertainty still exists about the origin of the high concentrations of trace elements in rock-glacier ice in the Central Eastern Alps (Colombo et

al., 2018a). However, during the HD period, Ni concentrations at RG3 exceeded the European guideline values for drinking water by a factor of two (Council of the European Union, 1998).

Isotopes, EC, pH, major ions and trace elements measured at RG3 were grouped within a PCA to provide an overview of the characteristics of the rock-glacier discharge into the pond. Figure 4 shows loading and score combined in a plot of the first two principal components. The bottom and left axes represent the scores of the analysis, whereas the top and right axes show factor loadings. The black and red dots represent sampling dates with reference to the first pair of axes, while the lengths of the arrows refer to the second-factor loadings. Factor loadings, representing the weightings of variables into each component, are the key to understanding the underlying nature of a particular factor. PCA revealed two main directions of variation, with Axis 1 explaining 47 % of the total variance and Axis 2 explaining an additional 22 %. An examination of the inter-set correlations of variables, together with the position and length of the arrows, revealed that the strongest direction of variation (Axis 1) was primarily a gradient of EC, major ions (SO_4^{2-}, NO_3^-, Mg^{2+}, Ca^{2+}), pH and isotopes ($\delta^{18}O$, δ^2H, d_{excess}). These variables had positive correlations with PCA Axis 1 (Fig. 4) and to each other (Tab. 4) and plotting towards the right of the ordination. Ni, Mn, and Co were highly correlated each other and with NO_3^- but not correlated with other major ions (SO_4^{2-}, Mg^{2+}, Ca^{2+}) (Tab. 4). Na^+ and K^+ were negatively correlated with trace elements and NO_3^- (Tab. 4), and plotted along the PCA Axis 2 (Fig. 4). From the PCA, it is possible to observe that the samples collected during the HD period (red dots in Fig. 4) plotted almost exclusively on the right side of the first ordination (Fig. 4), indicating that these dates were characterised by higher concentrations of some major ions (SO_4^{2-}, NO_3^-, Mg^{2+}, Ca^{2+}) and trace elements, and isotopically-enriched. By contrast, some dates (9, 15, and 20 July 2015) are plotted on the left side of the first ordination and they partially influenced the second direction of variation (Fig. 4), indicating higher concentrations in trace elements but lower major-ion concentrations, as observed at the beginning of the ice-free season 2015 (Fig. 2 and 3).

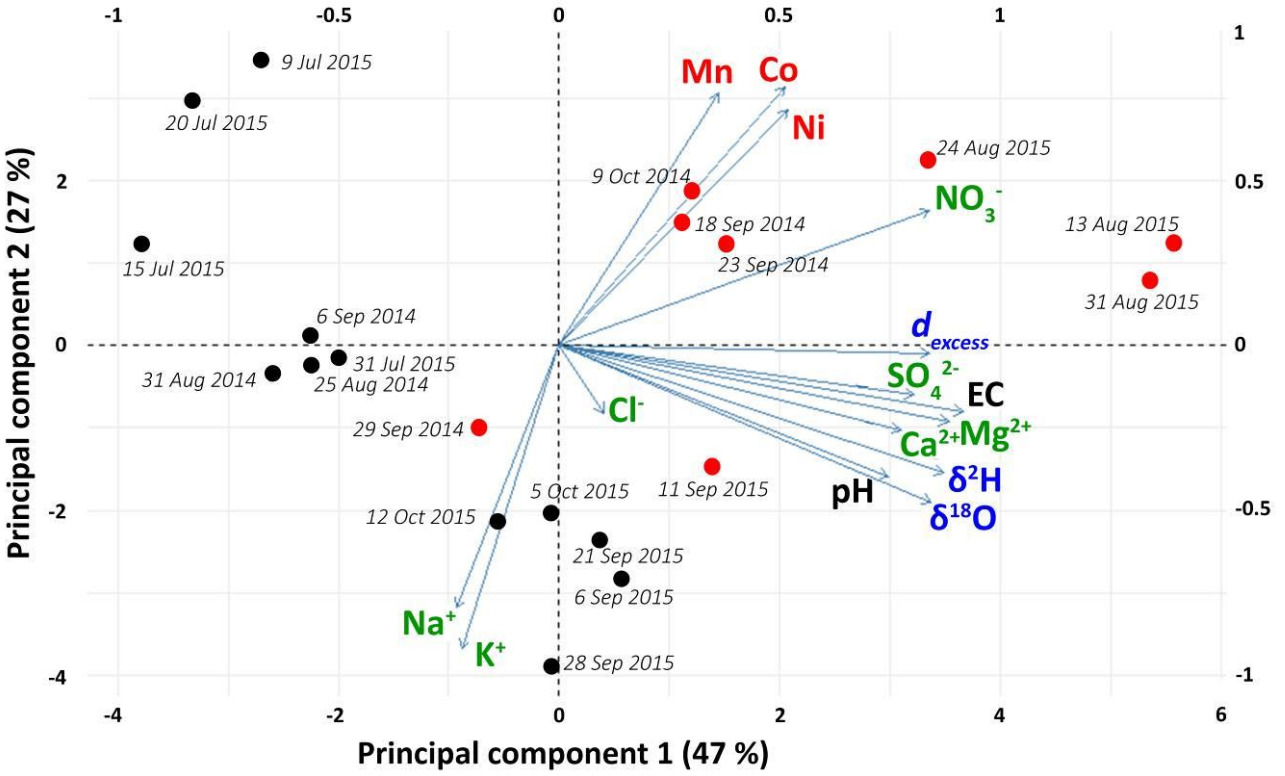

Figure 4 - Summary of results: PCA among isotopes (blue labels), EC and pH (black labels), major ions (green labels) and trace elements (red labels) of 20 sampling dates in which all variables were measured at RG3. Black and red dots indicate the sampling dates during periods of low-discharge (LD) and high-discharge (HD), respectively.

	EC	pH	SO_4^{2-}	NO_3^-	Cl^-	Mg^{2+}	Ca^{2+}	Na^+	K^+	Ni	Mn	Co	d_{excess}	$\delta^{18}O$	$\delta^{2}H$
EC	1														
pH	0.79***	1													
SO_4^2	0.91***	0.68***	1												
NO_3^-	0.65***	0.41*	0.57***	1											
Cl^-	0.08	0	0.16	0.13	1										
Mg^{2+}	0.80***	0.67***	0.73***	0.60***	0.23	1									
Ca^{2+}	0.74***	0.56***	0.61***	0.42*	0.04	0.88***	1								
Na^+	-0.10	0.15	-0.01	-0.47**	0.47**	0.02	-0.06	1							
K^+	-0.03	0.23	-0.07	-0.56**	0.11	-0.03	-0.01	0.78***	1						
Ni	0.30	0.02	0.29	0.69***	0.12	0.36	0.26	-0.58***	-0.76***	1					
Mn	0.18	0.07	0.21	0.65***	-0.01	0.03	-0.12	-0.50**	-0.67***	0.70***	1				
Co	0.26	0.13	0.27	0.68***	-0.09	0.34	0.26	-0.69***	-0.82***	0.80***	0.78***	1			
d_{excess}	0.69***	0.60***	0.53**	0.78***	-0.04	0.60***	0.48**	-0.18	-0.07	0.33	0.41*	0.35	1		
$\delta^{18}O$	0.80***	0.76***	0.61***	0.53**	0.16	0.82***	0.76***	0.12	0.26	0.11	-0.09	0.03	0.79***	1	
$\delta^{2}H$	0.80***	0.76***	0.61***	0.60***	0.10	0.80***	0.72***	0.04	0.19	0.16	0.02	0.11	0.86***	0.99***	1

Table 4 - Correlation matrix for measured variables of 20 sampling dates in which all variables were measured. Negative correlation coefficients mean inverse relationship. *, **, and * indicates significant correlation at p<0.1, p<0.05 and p<0.01, respectively.**

4.4 Conceptual model of solute export

We propose a conceptual model for explaining the main processes driving the export of solutes from the Col d'Olen Rock Glacier into the adjacent pond. It is based on inference since we rely on surface water measurements rather than direct measurement of water inside the rock glacier, and surface observations rather than knowledge of the internal structure of the rock glacier. Nevertheless, we believe that it has value despite these uncertainties, as it connects differing lines of evidence and may facilitate the generation and testing of new hypotheses. Regarding the internal structure of the rock glacier, fine-grained material is assumed to gradually become abundant with increasing depth, and close to the permafrost table, fines are predominant (Haeberli et al., 2006). An inner sediment-ice matrix is hypothesised (Haeberli, 1985; Barsch, 1988; Haeberli et al., 2006).

Before the beginning of the ice-free season, snowmelt is the dominant water source, depleted in isotopes and solute-diluted. When the ice-free season begins, higher concentrations of trace elements can be found in the pond (e.g., 9 July 2015), possibly due to mobilised trace elements in snowmelt or as a result of the ice cover on the pond for months during the winter that could result in increased concentrations of free metal ions (Fig. 5a). At this time, the 0 °C isotherm is near the surface (Fig. 5a) (cf., Williams et al., 2006).

Later in the ice-free season, the active layer is partially thawed and the remaining snowmelt (from long-lasting snow patches in hollows between and underneath boulders) flows through it. Near-surface ice, derived from snowmelt refrozen in the active layer, might also melt. The frozen core is well below 0 °C and at the same time, unfrozen water can exist as films on the surfaces of fine sediment particles (Williams and Smith, 1989; Rempel, 2012). This unfrozen water is geochemically-enriched due to solute expulsion during ice growth (Konrad and McCammon, 1990). At low temperatures, the permeability of the sediment-ice matrix is reduced due to the freezing of water and the decreased thickness of liquid films around sediment particles (Burt and Williams,

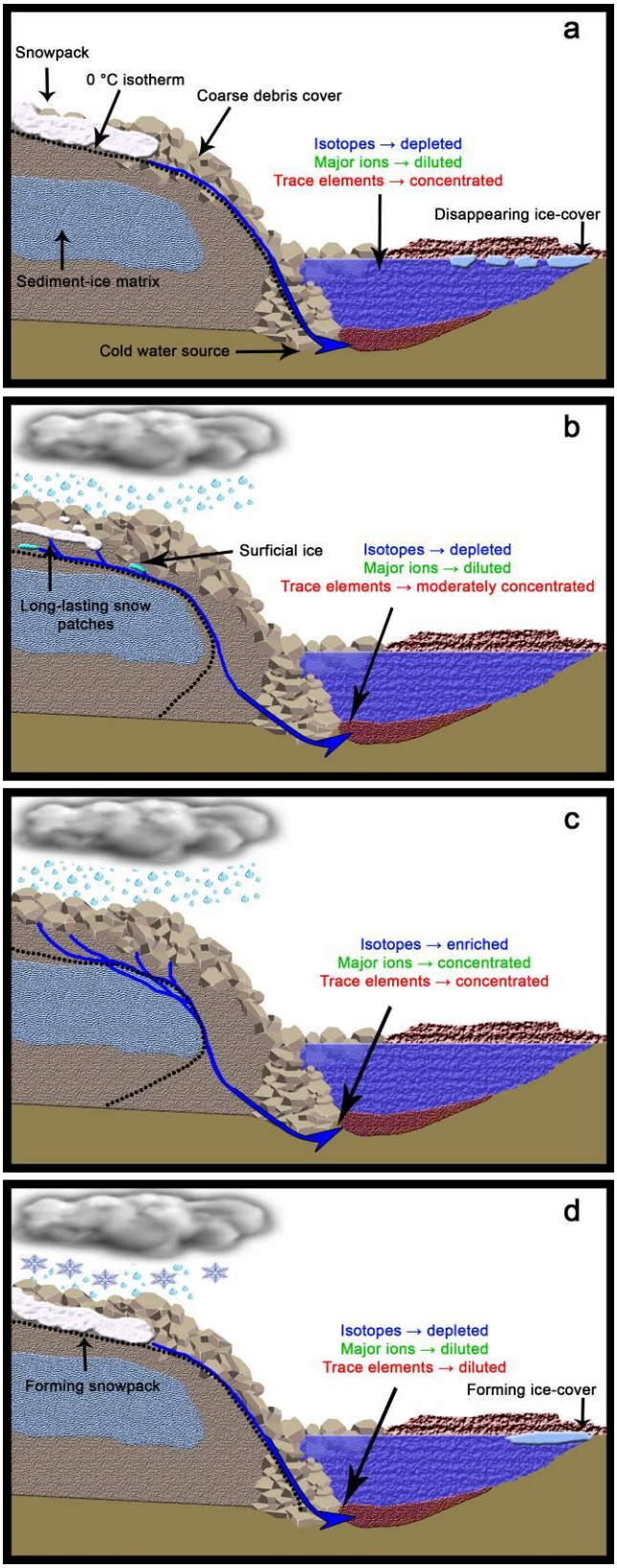

Figure 5 - Conceptual scheme of the hypothesised internal structure of the rock glacier and main processes driving the export of solutes into the marginal pond (modified from Colombo et al., 2018b).

(a) At the beginning of the ice-free season, the chemical characteristics of the water in the pond are mainly driven by snowmelt, which is depleted in isotopes and solute-diluted. High trace-element concentrations are found in the pond, possibly due to snowmelt mobilisation and/or prolonged winter ice-coverage of the pond. The 0 °C isotherm (black dotted line) is surficial. (b) Later in the ice-free season, the 0 °C isotherm extends into the rock glacier; the frozen core remains well below 0 °C and some unfrozen water exists within it. The rock-glacier discharge is generally low or moderate, and it mainly derives from long-lasting snow patches and surficial ice, resulting in isotopically-depleted water diluted in major ions. In this thermal condition, the percolating surficial water is not able to infiltrate into the rock-glacier core to mobilise solutes. Rainfall can cause moderate increases in trace-element concentrations, given their higher potential for export from the interior of the rock glacier. (c) After the snowmelt depletion and with the progression of the rock-glacier thawing, the 0 °C isotherm is deeper within the rock glacier, and the temperature of the uppermost zone of the internal sediment-ice matrix rises, causing a higher amount of unfrozen water; some ice might melt. In this thermal condition, rain is able to infiltrate into the rock-glacier core, and isotopically- and geochemically-enriched icemelt can be flushed, with concomitant increases in the rock-glacier discharge and the solute export. (d) Towards the end of the ice-free season, air temperature is negative or close to 0 °C for days and the 0 °C isotherm is surficial. Precipitation can occur in form of rain and snow, with the snowpack that can start forming. In this thermal condition, the rock-glacier discharge is low, isotopically-depleted and solute-diluted. Heterogeneity beyond this simplified model is like to exist inside the rock glacier.

1976). Meltwater from snow and near-surface ice at this time may percolate through the rock glacier in the voids created by the larger clast material, and infiltrating water likely flows mostly near and around the perennially frozen core. The 0 °C isotherm extends into the rock glacier (Fig. 5b) (cf., Williams et al., 2006). Minor amounts of internal meltwater can be exported after rainfall periods, which might be able to modify the thermal properties of the active layer (Iijima et al.,

2010), enhancing water percolation and ice melting. This association of source waters leads to a rather depleted isotopic signature and similar major-ion concentrations at all sampling points in the pond, with single concentration increase discrepancies at RG3 for easily exportable trace elements from the sediment-ice matrix after rainfall periods (e.g., July 2015).

After the snowmelt depletion and with the progression of the thawing season, the ground temperature rises and the temperature of the uppermost zone of the internal sediment-ice matrix rises as well. This leads to an increase in its permeability and in the amount of contained unfrozen water, even if still below 0 °C (melting point depression) (Williams and Smith, 1989; Kurylyk and Watanabe, 2013). The 0 °C isotherm might also extend into the frozen core, and some ice might melt. The internal ice is then in contact with a significant amount of liquid water and isotopic enrichment can be caused by melt/freeze episodes (Steig et al., 1998; Williams et al. 2006). Water in contact with newly-eroded mineral surfaces causes chemical weathering, further increasing the elemental products in the liquid water. Then, isotopically-enriched and elementally-depleted subsurface flow of infiltrated rainwater flushes this isotopically- and elementally-enriched icemelt, finally entering into the pond at RG3 (e.g., from mid-August to mid-September 2015) (Fig. 5c). Higher permeability of the sediment-ice matrix further allows the percolating rain to infiltrate in it (Haeberli et al. (2006) suggest that precipitation can infiltrate up to 0.5 m into rock glacier ice), enhancing the export of the available stored solutes. Moreover, water infiltrating into the frozen core might be further enhanced by the dilatancy effect due to warming ground temperature and melting ice in the creeping rock glacier (Arenson et al., 2002; Arenson and Palmer, 2005). Nitrate export from the rock glacier increases too, due to the flushing of microbially-active sediments.

Towards the end of the ice-free season, after days of atmospheric temperature negative or close to 0 °C, the active layer is freezing back. The 0 °C isotherm is more surficial. Precipitation can be in form of both rain and snow, and snowpack can start forming on the rock glacier. In this thermal condition, the rock-glacier discharge is low, leading to a relatively low export of solutes and, at

some point, the cold water source freezes/dries-out and no further export of water and solutes occurs (e.g., from mid-September to the end of the ice-free season 2015) (Fig. 5d).

4.5 Potential environmental implications and research perspectives

As demonstrated in this work, after winter snowmelt depletion, rainfall events facilitate the export of solutes previously stored a rock-glacier. In the Northern Hemisphere, snow cover extent in spring (March, April) has undergone significant reduction over the period 1922-2010 (Brown and Robinson, 2011). Contextually, a significant air temperature increase (1.26 °C) at hemispheric scale has been found at mid-latitudinal land areas (40°-60°N) (Brutel-Vuilmet et al., 2016). In the North-Western Italian Alps between 1961 and 2010 the weather stations located above 1600 m a.s.l. presented an increase in air temperature (Acquaotta et al., 2015). Moreover, Terzago et al. (2012, 2013) outlined a significant decrease of snow depth over seasonal (November-May) time scale, and Fratianni et al. (2015) reported significant decreases in fresh snow, causing a shift of the snowmelt in spring as also reported for the Swiss Alps (Klein et al., 2016). As global climate models generally predict a continuous increase in air temperature during the coming decades, suggesting that moisture availability under warmer scenarios is likely to increase summer rainfall (IPCC, 2013), it is possible to predict an increase in solute flushing from rock glaciers. However, the impacts of this process on surface-water characteristics will likely be dependent on the ratio of rock-glacier size to catchment area, frozen core characteristics and dimensions, characteristics of the rock-glacier internal hydrological system, and lithological setting. For instance, as observed in this work, the rock glacier is approximately 11 % of the total catchment area, thus the other pond inflows (e.g., runoff from non-rock-glaciated zones of the catchment) diluted the enrichment of solutes provided by the rock glacier. Higher rock glacier/catchment area ratios (Thies et al., 2007), high elemental concentrations in rock-glacier ice (Krainer et al., 2011, 2015), and the occurrence of acid rock drainage (Ilyashuk et al., 2014, 2017) will likely have stronger impacts on surface-water

characteristics in other environments. Finally, this study shows the effect of rain on solute flushing from rock glaciers, a process that has been previously described for permafrost in the Arctic.

This study suggests potential future research directions. Considering the limited number of studies on the effects of rock-glacier thawing on downstream water quality, the establishment of frequent monitoring for key chemical analytes in surface water will provide greater statistical power to detect changes in solute levels, especially considering elements that are dangerous for drinking water and ecosystem health. In this context, what duration will the transient effects of the increased geochemical contribution of rock glaciers have? Will these effects subside after a few decades when rock glaciers become inactive or relict, or will the sediment bodies continue to supply higher solute levels? Finally, other debris-cover features can be interested by the presence of permafrost containing a significant amount of ground ice such as talus slopes (Lambiel and Pieracci, 2008; Scapozza et al., 2011), which are omnipresent in mountain landscapes (Sass, 2006). Should we expect the same behaviour evidenced in rock glaciers for these typical mountain features?

5. Conclusions

Several hypotheses to explain how weather and climate drive the export of solute (major ions and trace elements) enriched water from active rock glaciers have been published but remain underpinned and tested with sparse data, only. This study complements previous efforts by reporting weekly observations of a wide range of variables (air temperature, snowmelt, rainfall, water temperature as a proxy of rock-glacier discharge, stable water isotopes, major ions and selected trace elements) characterising a rock glacier-pond system. From the results and discussion, the following conclusions are drawn:

1) Periods of high discharge from this rock glacier were synchronous with periods of enhanced export of major ions and trace elements.

2) Rainfall events have been found to be the primary meteorological driver of the rock-glacier discharge and, therefore, the solute export from the landform during the ice-free season.
3) A conceptual model has been proposed for describing the potential mechanisms responsible for the solute export from the rock glacier. At the beginning of the ice-free season, snowmelt runoff, isotopically-depleted and diluted in major ions, is the dominant water source. Snowmelt mobilisation and/or prolonged winter ice-coverage might be responsible for the high trace-element concentrations in the pond. During the ice-free season, after the winter snowpack melting and prolonged periods of atmospheric temperature above 0 °C, rain can infiltrate in the rock-glacier core, likely flushing the isotopically- and geochemically-enriched icemelt. This causes concomitant increases in the rock-glacier discharge and the solute export (SO_4^{2-}, Mg^{2+}, Ca^{2+}, Ni, Mn, Co). Moreover, flushing of microbially-active sediments can cause increases in NO_3^- export.

With projected reductions in snow cover duration and increases in air temperature and summer rainfall in the Northern Hemisphere and, specifically, in the Alps, an increase in solute flushing from rock glaciers is likely to occur in the future. The characteristics of catchments (e.g., ratio of rock-glacier size to catchment area, lithological setting) and of rock glaciers (e.g., frozen core structure and dimensions, hydrological system properties) will likely influence the timing and magnitude of the impacts of rock-glacier thawing. Thus, additional investigations on rock-glacier dynamics and internal structure might help in extending our knowledge on rock-glacier thawing impacts on surface water and testing hypotheses on the main processes driving the export of solutes from this typical mountain landform.

Acknowledgments

Nicola Colombo and Franco Salerno equally contributed to this paper. We would like to thank Elena Serra, Elisa Giaccone, Ilaria Mania, Emanuele Pintaldi, Davide Viglietti, Marco Prati, Marco

Bacenetti, Diego Guenzi, Cristina Viani and Gioachino Roberti for their help in data acquisition, fieldwork and laboratory activities. We are also grateful for the support given by Luigi Perotti (Department of Earth Sciences, University of Turin, Italy), Holly Hughes (Department of Geography, University of Colorado, Boulder, USA), Daniel Said Pullicino (Department of Agricultural, Forest and Food Sciences, University of Turin, Italy), Lino Judica and Adriana Bovio (Territorial Laboratory of Environmental Education, University of Turin, Italy), Ernesto Colombo, Lorena Bulla and Carina Schuh. We give special thanks to the family Beck-Peccoz, Consorzio di Miglioramento Fondiario di Gressoney (Aosta) and MonteRosa-ski. We greatly acknowledge the support in the isotopic analyses by Mark Williams (Department of Geography, University of Colorado, Boulder, USA) and the valuable suggestions provided by Karl Krainer (Innsbruck). This research has been partially developed in the framework of the PRIN 2010-11 (funded project of the Italian Ministry for Education and Research) named "Dinamica dei sistemi morfoclimatici in risposta ai cambiamenti globali e rischi geomorfologici indotti" (coord. Prof. Carlo Baroni). Finally, the editor and anonymous reviewers provided valuable feedback and input during the review of this manuscript.

References

Acquaotta, F., Fratianni, S., Garzena, D. (2015). Temperature changes in the North-Western Italian Alps from 1961 to 2010. Theoretical and Applied Climatology, 122: 619-634.

Adrian, R., Reilly, C.M.O., Zagarese, H., Baines, S.B., Hessen, D.O., Keller, W., Livingstone, D.M., Sommaruga, R., Straile, D., Van Donk, E., Weyhenmeyer, G.A., Winder, M. (2009). Lakes as sentinels of climate change. Limnology and Oceanography, 54(6): 2283-2297.

Anderson, D., Tice, A., McKim, H. (1973). The unfrozen water and the apparent specific heat capacity of frozen soils. Proceedings of the Second International Conference on Permafrost, 289-295.

Arenson, L.U., Hoelzle, M., Springman, S. (2002). Borehole deformation measurements and internal structure of some rock glaciers in Switzerland. Permafrost and Periglacial Processes, 13: 117-135.

Arenson, L.U., Palmer, A.C. (2005). Rock glaciers, fault gouge and asphalt. Hard particles in a nonlinear creeping matrix. Cold Regions Science and Technology, 43: 117-127.

Bagard, M.L., Chabaux, F., Pokrovsky, O.S., Viers, J., Prokushkin, A.S., Stille, P., Rihs, S., Schmit, A.D., Dupre, B. (2011). Seasonal variability of elements fluxes in two Central Siberian rivers draining high latitude permafrost dominated areas. Geochimica et Cosmochimica Acta, 75: 3335-3357.

Balestrini, R., Polesello, S., Sacchi, E. (2014). Chemistry and isotopic composition of precipitation and surface waters in Khumbu valley (Nepal Himalaya): N dynamics of high elevation basins. Science of the Total Environment, 485-486: 681-692.

Baltensperger, U., Gaggeler, H., Gloor, M., Hoehn, E., and Keil, R. (1990). Chemical composition. Pilot Analyses of Permafrost Cores from the Active Rock Glacier Murtèl, Piz Corvatsch, Eastern Swiss Alps. Workshop Report, Arbeitsheft VAW/ETHZ.

Barker, A.J., Douglas, T.A., Jacobson, A.D., McClelland, J.W., Ilgen, A.G., Khosh, M.S., Lehn, G.O., Trainor, T.P. (2014). Late season mobilization of trace metals in two small Alaskan arctic watersheds as a proxy for landscape scale permafrost active layer dynamics. Chemical Geology, 381: 180-193.

Barnes, R.T., Williams, M.W., Parman, J.N., Hill, K., Caine, N. (2014). Thawing glacial and permafrost features contribute to nitrogen export from Green Lakes Valley, Colorado Front Range, USA. Biogeochemistry, 117: 413-430.

Baron, J.S., Schmidt, T.M., Harman, M.D. (2009). Climate-induced changes in high-elevation stream nitrate dynamics. Global Change Biology, 15(7): 1777-1789.

Barsch, D. (1988). Rockglaciers. [Ed.] Clark, M.J, Advances in Periglacial Geomorphology. Wiley,

New York, 69-90.

Barsch, D. (1996). Rockglaciers: Indicators for the Present and Former Geoecology in High Mountain Environments. Springer-Verlag: Berlin-Heidelberg.

Baumeister, J.L., Hausrath, E.M., Olsen, A.A., Tschauner, O., Adcock, C.T., Metcalf, R.V. (2015). Biogeochemical weathering of serpentinites: An examination of incipient dissolution affecting serpentine soil formation. Applied Geochemistry, 54: 74-84.

Berger, J., Krainer, K., Mostler, W. (2004). Dynamics of an active rockglacier (Ötztal Alps, Austria). Quaternary Research, 62: 233-242.

Blodau, C., Mayer, B., Peiffer, S., Moore, T.R. (2007). Support for an anaerobic sulfur cycle in two Canadian peatland soils. Journal of Geophysical Research, 112(G2): G02004, doi:org/10.1029/2006JG000364.

Blumstock, M., Tetzlaff, D., Malcolm, I.A., Nuetzmann, G., Soulsby, C. (2015). Baseflow dynamics: Multi-tracer surveys to assess variable groundwater contributions to montane streams under low flows. Journal of Hydrology, 527: 1021-1033.

Brooks, R.R. (1987). Serpentine and Its Vegetation. Dioscorides Press, Portland.

Brown, R.D., Robinson, D.A. (2011). Northern Hemisphere spring snow cover variability and change over 1922-2010 including an assessment of uncertainty. The Cryosphere, 5: 219-229.

Brutel-Vuilmet, C., Ménégoz, M., Krinner, G. (2013). An analysis of present and future seasonal Northern Hemisphere land snow cover simulated by CMIP5 coupled climate models. The Cryosphere, 7: 67-80.

Buchli, T., Merz, K., Zhouc, X., Kinzelbachc, W., Springman, S.H. (2013). Characterization and monitoring of the Furggwanghorn Rock Glacier, Turtmann Valley, Switzerland: Results from 2010 to 2012. Vadose Zone Journal, 12(1), doi:10.2136/Vzj2012.0067.

Burger, K.C., Degenhardt, J.J., Giardino, J.R. (1999). Engineering geomorphology of rock glaciers. Geomorphology, 31: 93-132.

Burt, T.P., Williams, P.J. (1976). Hydraulic conductivity in frozen soils. Earth Surface Processes, 1(3): 349-360.

Catalan, J., Camarero, L., Felip, M., Pla, S., Ventura, M., Buchaca, T., Bartumeus, F., de Mendoza, G., Miró, A., Casamayor, E.O., Medina-Sánchez, J.M., Bacardit, M., Altuna, M., Bartrons, M., De Quijano, D.D. (2006). High mountain lakes: Extreme habitats and witnesses of environmental changes. Limnetica, 25(1-2): 551-584.

Clow, D.W., Drever, J. (1996). Weathering rates as a function of flow through an alpine soil. Chemical Geology, 132(1-4): 131-141.

Clow, D.W., Mast, M.A. (2010). Mechanisms for chemostatic behavior in catchments: Implications for CO_2 consumption by mineral weathering. Chemical Geology, 269: 40-51.

Colombo, N., Salerno, F., Gruber, S., Freppaz, M., Williams, M., Fratianni, S., Giardino, M. (2018a). Review: Impacts of permafrost degradation on inorganic chemistry of surface fresh water. Global and Planetary Change, Global and Planetary Change, 162: 69-83.

Colombo, N., Sambuelli, L., Comina, C., Colombero, C., Giardino, M., Gruber, S., Viviano, G., Vittori Antisari, L., Salerno, F. (2018b). Mechanisms linking active rock glaciers and impounded surface water formation in high-mountain areas. Earth Surface Processes and Landforms, 43(2): 417-431.

Council of the European Union (1998). Directive on the Quality of Water Intended for Human Consumption, 98/83/CE, Official Journal of the European Communities. European Union, Brussels.

Craig, H. (1961). Isotopic variations in meteoric waters. Science, 133: 1702-1703.

Dansgaard, W. (1964). Stable isotopes in precipitation. Tellus, 16: 436-468.

Fegel, T.S., Baron, J.S., Fountain, A.G., Johnson, G.F., Hall, E.K. (2016). The differing biogeochemical and microbial signatures of glaciers and rock glaciers. Journal of Geophysical Research, 121(3): 919-932.

Fratianni, S., Terzago, S., Acquaotta, F., Faletto, M., Garzena, D., Prola, M.C., Barbero, S. (2015). How snow and its physical properties change in a changing climate alpine context? Engineering Geology for society and territory, Springer, 1(11): 57-60.

Frey, K.E., McClelland, J.W. (2009). Impacts of permafrost degradation on arctic river biogeochemistry. Hydrological Processes, 23: 169-182.

Froehlich, H.L., Breuer, L., Frede, H., Huisman, J.A., Vach, K.B. (2008). Water source characterization through spatiotemporal patterns of major, minor and trace element stream concentrations in a complex, mesoscale German. Hydrological Processes, 2043(2007): 2028-2043.

Gadek, B., Leszkiewicz, J. (2010). Influence of snow cover on ground surface temperature in the zone of sporadic permafrost, Tatra Mountains, Poland and Slovakia. Cold Regions Science and Technology, 60(3): 205-211.

Gasco, I., Borghi, A., Gattiglio, M. (2011). P-T Alpine metamorphic evolution of the Monte Rosa nappe along the Piedmont Zone boundary (Gressoney Valley, NW Italy). Lithos, 127(1-2): 336-353.

Geiger, S.T., Daniels, J.M., Miller, S.N., Nicholas, J.W. (2014). Influence of rock glaciers on stream hydrology in the La Sal Mountains, Utah. Arctic, Antarctic, and Alpine Research, 46(3): 645-658.

Godsey, S.E., Kirchner, J.W., Clow, D.W. (2009). Concentration-discharge relationships reflect chemostatic characteristics of US catchments. Hydrological Processes, 23(13): 1844-1864.

Goulsbra, C., Evans, M., Lindsay, J. (2014). Temporary streams in a peatland catchment: pattern, timing, and controls on stream network expansion and contraction. Earth Surface Processes and Landforms, 39(6): 790-803.

Guzzella, L., Salerno, F., Freppaz, M., Roscioli, C., Pisanello, F., Poma, G. (2016). POP and PAH contamination in the southern slopes of Mt. Everest (Himalaya, Nepal): Long-range

atmospheric transport, glacier shrinkage, or local impact of tourism? Science of the Total Environment, 544: 382-390.

Haeberli, W. (1985). Creep of mountain permafrost: internal structure and flow of alpine rock glaciers. Mitt. ETH Zurich 77.

Haeberli, W., Hallet, B., Arenson, L.U., Elconin, R., Humlum, O., Kääb, A., Kaufmann, V., Ladanyi, B., Matsuoka, N., Springman, S., Vonder Mühll, D. (2006). Permafrost creep and rock glacier dynamics. Permafrost and Periglacial Processes, 17: 189-214.

Haeberli, W., Kääb, A., Wagner, S., Geissler, P., Haas, J. N., Glatzel-Mattheier, H., Wagenbach, D., and Vonder Mühll, D. (1999). Pollen analysis and ^{14}C-age of moss remains recovered from a permafrost core of the active rock glacier Murtèl/Corvatsch (Swiss Alps): geomorphological and glaciological implications. Journal of Glaciology, 45(149): 1-8.

Handy, M.R., Schmid, S.M., Bousquet, R., Kissling, E., Bernoulli, D. (2010). Reconciling plate-tectonic reconstructions of Alpine Tethys with the geological-geophysical record of spreading and subduction in the Alps. Earth-Science Reviews, 102(3-4): 121-158.

Hanson, S., Hoelzle, M. (2004). The thermal regime of the active layer at the Murtèl Rock Glacier based on data from 2002. Permafrost and Periglacial Processes, 15: 273-282.

Harris, S.A., Wayne, K., Blumenstengel, D., Cook, H., Krouse, R., Whitley, G. (1994). Comparison of the water drainage from an active near-slope rock glacier and a glacier, St. Elias Mountains, Yukon Territory. Erdkunde, 48: 81-91.

Hinkel, K.M., Paetzold, F., Nelson, F.E., Bockheim, J.G. (2001). Patterns of soil temperature and moisture in the active layer and upper permafrost at Barrow, Alaska: 1993-1999. Global and Planetary Change, 29: 293-309.

Holmer, M., Storkholm, P. (2001). Sulphate reduction and sulphur cycling in lake sediments: a review. Freshwater Biology, 46: 431-451.

Iijima, Y., Fedorov, A.N., Park, H., Suzuki, K., Yabuki, H., Maximov, T.C., Ohata, T. (2010).

Abrupt increases in soil temperatures following increased precipitation in a permafrost region, Central Lena River Basin, Russia. Permafrost and Periglacial Processes, 21: 30-41.

Ilyashuk, B.P., Ilyashuk, E.A., Psenner, R., Tessadri, R., Koinig, K.A. (2014). Rock glacier outflows may adversely affect lakes: Lessons from the past and present of two neighboring water bodies in a crystalline-rock watershed. Environmental Science and Technology, 48(11): 6192-6200.

Ilyashuk, B.P., Ilyashuk, E.A., Psenner, R., Tessadri, R., Koinig, K.A. (2017). Rock glaciers in crystalline catchments: hidden permafrost-related threats to alpine headwater lakes. Global Change Biology, doi:10.1111/gcb.13985.

IPCC (2013). Climate Change 2013: The Physical Science Basis. Contribution of Working Group I to the Fifth Assessment Report of the Intergovernmental Panel on Climate Change. Cambridge University Press, Cambridge, United Kingdom and New York, NY, USA.

Jeelani, Gh., Bhat, N.A., Shivanna, K. (2010). Use of $\delta^{18}O$ tracer to identify stream and spring origins of a mountainous catchment: A case study from Liddar watershed, Western Himalaya, India. Journal of Hydrology, 393: 257-264.

Johnsen, S.J., White, J.W.C. (1989). The origin of arctic precipitation under present and glacial conditions. Tellus, 41(B): 452-468.

Johnson, P.G. (1981). The structure of a talus-derived rock glacier deduced from its hydrology. Canadian Journal of Earth Sciences, 18: 1422-1430.

Jones, D.B., Harrison, S., Anderson, K., Betts, R.A. (2018). Mountain rock glaciers contain globally significant water stores. Scientific Reports, 8(1): 2834, doi:10.1038/s41598-018-21244-w.

Jonsson, C.E., Leng, M.J., Rosqvist, G.C., Seibert, J., Arrowsmith, C. (2009). Stable oxygen and hydrogen isotopes in sub-Arctic lake waters from northern Sweden. Journal of Hydrology, 376: 143-151.

Jørgensen, B.B. (1988). Ecology of the sulphur cycle: oxidative pathways in the sediment. In: The

Nitrogen and Sulphur Cycles, [Eds.]. Cole, J.A., Ferguson, S.J., Cambridge University Press, Cambridge, 31-63.

Jørgensen, B.B. (1990). The sulfur cycle of freshwater sediments: Role of thiosulfate. Limnology and Oceanography, 35: 1329-1342.

Juliussen, H., Humlum, O., Kristensen, L., Christiansen, H.H. (2008). Thermal Processes in the Active Layer of the Larsbreen Rock Glaciers, Central Spitsbergen, Svalbard. Proceedings of the Ninth International Conference on Permafrost, 877-882.

Klein, G., Vitasse, Y., Rixen, C., Marty, C., Rebetez, M. (2016). Shorter snow cover duration since 1970 in the Swiss alps due to earlier snowmelt more than to later snow onset. Climatic Change, 139(3): 637-649.

Konrad, J.M., McCammon, A.W. (1990). Solute portioning in freezing soils. Canadian Geotechnical Journal, 27(6): 726-736.

Krainer, K., Bressan, D., Dietre, B., Haas, J.N., Hajdas, I., Lang, K., Mair, V., Nickus, U., Reidl, D., Thies, H., Tonidandel, D. (2015). A 10,300-year-old permafrost core from the active rock glacier Lazaun, southern Ötztal Alps (South Tyrol, northern Italy). Quaternary Research, 83(2): 324-335.

Krainer, K., Mostler, W. (2001a). Aktive Blockgletscher als Transportsysteme für Schuttmassen im Hochgebirge: Der Reichenkar Blockgletscher in den westlichen Stubaier Alpen. Geoforum Umhausen, 1: 28-43.

Krainer, K., Mostler, W. (2001b). Der aktive Blockgletscher im Hinteren Langtal Kar, Gößnitz Tal (Schober Gruppe, Nationalpark Hohe Tauern). Wissenschaftliche Mitteilungen aus dem Nationalpark Hohe Tauern, 6: 139-168.

Krainer, K., Mostler, W. (2002). Hydrology of Active Rock Glaciers: Examples from the Austrian Alps. Arctic, Antarctic, and Alpine Research, 34(2): 142-149.

Krainer, K., Mostler, W., Spötl, C. (2007). Discharge from active rock glaciers, Austrian Alps: A

stable isotope approach. Austrian Journal of Earth Sciences, 100: 102-112.

Krainer, K., Mussner, L., Behm, M., Hausmann, H. (2012). Multi-disciplinary investigation of an active rock glacier in the Sella Group (Dolomites; Northern Italy). Austrian Journal of Earth Sciences, 105(2): 48-62.

Krainer, K., Nickus, U., Thies, H., Tessadri, R. (2011). Geochemical analyses of permafrost ice and of permafrost water springs. PermaNET Project report, WP7.

Kummert, M., Delaloye, R., Braillard, L. (2017) Erosion and sediment transfer processes at the front of rapidly moving rock glaciers: Systematic observations with automatic cameras in the western Swiss Alps. Permafrost and Periglacial Processes, doi.org/10.1002/ppp.1960.

Kurylyk, B.L., Watanabe, K. (2013). The mathematical representation of freezing and thawing processes in variably-saturated, non-deformable soils. Advances in Water Resources, 60: 160-177.

Lambiel, C., Pieracci, K. (2008). Permafrost distribution in talus slopes located within the alpine periglacial belt, Swiss Alps. Permafrost and Periglacial Processes, 19: 293-304.

Lamhonwah, D., Lafrenière, M.J., Lamoureux, S.F., Wolfe, B.B. (2017). Evaluating the hydrological and hydrochemical responses of a High Arctic catchment during an exceptionally warm summer. Hydrological Processes, 31(12): 2296-2313.

Ley, R.E., Schmidt, S.K. (2002). Fungal and bacterial responses to phenolic compounds and amino acids in high altitude barren soils. Soil Biology and biochemistry, 34: 989-996.

Ley, R.E., Williams, M.W., Schmidt, S.K. (2004). Microbial population dynamics in an extreme environment: controlling factors in talus soils at 3,750 m in the Colorado Rocky Mountains. Biogeochemistry 68 (3), 313-335.

Luetschg, M., Lehning, M., Haeberli, W. (2008). A sensitivity study of influencing warm/thin permafrost in the Swiss Alps. Journal of Glaciology, 54: 696-704.

Magnani, A., Viglietti, D., Balestrini, R., Williams, M.W., Freppaz, M. (2017). Contribution of

deeper soil horizons to N and C cycling during the snow-free season in alpine tundra, NW Italy. Catena, 155: 75-85.

Millar, C.I., Westfall, R.D. (2008). Rock glaciers and related periglacial landforms in the Sierra Nevada, CA, USA: inventory, distribution, and climatic relationships. Quaternary International, 188: 90-104.

Millar, C.I., Westfall, R.D., Delany, D.L. (2013). Thermal and hydrologic attributes of rock glaciers and periglacial talus landforms: Sierra Nevada, California, USA. Quaternary International, 310: 169-180.

Monteith, J.L. (1985). Evaporation from land surfaces: progress in analysis and prediction since 1948. Proceedings of the National Conference on Advances in Evapotranspiration, 4-12.

Penman, H.L. (1948). Natural evaporation from open water, bare soil and grass. Proceeding of the Royal Meteorological Society, A193: 120-145.

Penna, D., Engel, M., Mao, L., Dell'Agnese, A., Bertoldi, G., Comiti, F. (2014). Tracer-based analysis of spatial and temporal variations of water sources in a glacierized catchment. Hydrology and Earth System Sciences, 18: 5271-5288.

R Development Core Team, R. (2011). R: A Language and Environment for Statistical Computing. (R. D. C. Team, Ed.) R Foundation for Statistical Computing, doi:10.1007/978-3-540-74686-7.

Rember, R., Trefry, J. (2004). Increased concentrations of dissolved trace metals and organic carbon during snowmelt in rivers of the Alaskan arctic. Geochimica et Cosmochimica Acta, 68: 477-489.

Rempel, A.W. (2012). Hydromechanical processes in freezing soils. Vadose Zone Journal, 11, doi:10.2136/vzj2012.0045.

Rist, A., Phillips, M. (2005). First results of investigations on hydrothermal processes within the active layer above alpine permafrost in steep terrain. Norsk Geografisk Tidsskrift-Norwegian Journal of Geography, 59: 177-183.

Roy, J.W., Hayashi, M. (2009). Multiple, distinct groundwater flow systems of a single moraine-talus feature in an alpine watershed. Journal of Hydrology, 373(1): 139-150.

Salerno, F., Gambelli, S., Viviano, G., Thakuri, S., Guyennon, N., D'Agata, C., Diolaiuti, G., Smiraglia, C., Stefani, F., Bocchiola, D., Tartari, G. (2014). High alpine ponds shift upwards as average temperatures increase: A case study of the Ortles-Cevedale mountain group (Southern Alps, Italy) over the last 50 years. Global and Planetary Change, 120: 81-91.

Salerno, F., Rogora, M., Balestrini, R., Lami, A., Tartari, G. A., Thakuri, S., Tartari, G. (2016). Glacier melting increases the solute concentrations of Himalayan glacial lakes. Environmental Science & Technology, 50(17): 9150-9160.

Salomons, W. (1995). Environmental impact of metals derived from mining activities: Processes, predictions, prevention. Journal of Geochemical Exploration, 51: 5-23.

Sass, O. (2006). Determination of the internal structure of alpine talus deposits using different geophysical methods (Lechtaler Alps, Austria). Geomorphology, 80: 45-58.

Scapozza, C., Lambiel, C., Baron, L, Marescot, L., Reynard, E. (2011). Internal structure and permafrost distribution in two alpine periglacial talus slopes, Valais, Swiss Alps. Geomorphology, 132(34): 208-221.

Schmid, M.O., Gubler, S., Fiddes, J., Gruber, S. (2012). Inferring snowpack ripening and melt-out from distributed measurements of near-surface ground temperatures. The Cryosphere, 6(5): 1127-1139.

Schreier, H., Omueti, J.A., and Lavkulich, L.M. (1987). Weathering processes of asbestos-rich serpentinitic sediments. Soil Science Society of America Journal, 51: 993-999.

Staub, B., Delaloye, R. (2016). Using near-surface ground temperature data to derive snow insulation and melt indices for mountain permafrost applications. Permafrost and Periglacial Processes, 28(1): 237-248.

Steck, A., Masson, H., Robyr, M. (2015). Tectonics of the Monte Rosa and surrounding nappes

(Switzerland and Italy): Tertiary phases of subduction, thrusting and folding in the Pennine Alps. Swiss Journal of Geosciences, 108: 3-34.

Steig, E.J., Fitzpatrick, J., Potter, N.J., Clark, D.H. (1998). The geochemical record in rock glaciers. Geografiska Annaler, 80: 277-286.

Storey, J., Choate, M., Lee, K. (2014). Landsat 8 operational land imager on-orbit geometric calibration and performance. Remote Sensing, 6(11): 11127-11152.

Tenthorey, G. (1992). Short communication: Perennial névés and the hydrology of rock glaciers. Permafrost and Periglacial Processes, 3: 247-252.

Tenthorey, G. (1993). Paysage géomorphologique du Haut-Val de Réchy (Valais, Suisse) et hydrologie liée aux glaciers rocheux. PhD thesis, University of Fribourg, Switzerland.

Terzago, S., Cremonini, R., Cassardo, C., Fratianni, S. (2012). Analysis of snow cover precipitation during the period 2000-09 and evaluation of a MSG/SEVIRI snow cover algorithm in SW Italian Alps. Geografia Fisica & Dinamica Quaternaria, 35: 91-99.

Terzago, S., Fratianni, S., Cremonini, R. (2013). Winter precipitation in Western Italian Alps (1926-2010): trends and connections with the North Atlantic/Arctic Oscillation. Meteorology and Atmospheric Physics, 704: 125-136.

Thies, H., Nickus, U., Tessadri, R., Psenner, R. (2007). Unexpected response of high Alpine Lake waters to climate warming. Environmental Science & Technology, 41, 7424-7429.

Thies, H., Nickus, U., Tolotti, M., Tessadri, R., Krainer, K. (2013). Evidence of rock glacier melt impacts on water chemistry and diatoms in high mountain streams. Cold Regions Science and Technology, 96: 77-85.

Tolotti, M., Forsstrom, L., Morabito, G., Thaler, B., Stoyneva, M., Cantonati, M., Šiško, M., Lotter, A. (2009). Biogeographical characterisation of phytoplankton assemblages in high altitude, and high latitude European lakes. Advances in Limnology, 62: 55-75.

Touhari, F., Meddi, M., Mehaiguene, M., Razack, M. (2014). Hydrogeochemical assessment of the

Upper Cheliff groundwater (North West Algeria). Environmental Earth Sciences, 73: 3043, doi:10.1007/s12665-014-3598-6.

Venables, W.N., Ripley, B.D. (2002). Modern Applied Statistics with S. Springer, New York.

Vithanage, M., Rajapaksha, A.U., Oze, C., Rajakaruna, N., Dissanayake, C.B. (2014). Metal release from serpentine soils in Sri Lanka. Environmental Monitoring and Assessment, 186(6): 3415-3429.

Vonk, J.E., Tank, S.E., Bowden, W.B., Laurion, I., Vincent, W.F., Alekseychik, P., Amyot, M., Billet, M.F., Canário, J., Cory, R.M., Deshpande, B.N., Helbig, M., Jammet, M., Karlsson, J., Larouche, J., MacMillan, G., Rautio, M., Walter Anthony, K.M., Wickland, K.P. (2015). Reviews and syntheses: Effects of permafrost thaw on Arctic aquatic ecosystems. Biogeosciences, 12: 7129-7167.

Walling, D.E., Webb, B.W. (1986). Solutes in river systems. [Ed.] Trudgill, S.T., Solute Processes, John Wiley & Sons, Chichester, 251-327.

Williams, M.W., Davinroy, T., Brooks, P.D. (1997). Organic and inorganic nitrogen pools in talus soils and water, Green Lakes Valley, Colorado Front Range. Hydrologic Processes, 11(13): 1747-1760.

Williams, M.W., Hood, E., Molotch, N.P., Caine, N., Cowie, R., Liu, F. (2015). The ‘teflon basin’ myth: hydrology and hydrochemistry of a seasonally snow-covered catchment. Plant Ecology & Diversity, 8(5-6): 639-661.

Williams, M.W., Knauf, M., Caine, N., Liu, F., Verplanck, P.L. (2006). Geochemistry and source waters of rock glacier outflow, Colorado Front Range. Permafrost and Periglacial Processes, 17(1): 13-33.

Williams, M.W., Knauf, M., Cory, R., Caine, N., Liu, N. (2007). Nitrate content and potential microbial signature of rock glacier outflow, Colorado Front Range. Earth Surface Processes and Landforms, 32: 1032-1047.

Williams, P.J., Smith, M.W. (1989). The frozen earth. Fundamentals of geocryology. Cambridge University Press, Cambridge.

Wirz, V., Gruber, S., Purves, R.S., Beutel, J., Gärtner-Roer, I., Gubler, S., Vieli, A. (2016). Short-term velocity variations of three rock glaciers and their relationship with meteorological conditions. Earth Surface Dynamics, 4: 103-123.

Woo, M. (2012). Permafrost hydrology. Springer-Verlag Berlin Heidelberg.

Wögrath, S., Psenner, R. (1995). Seasonal, annual and long-term variability in the water chemistry of a remote high mountain lake: Acid rain versus natural changes. Water, Air, and Soil Pollution, 85: 359-364.

Yuan, F.S., Sheng, Y.W., Yao, T.D., Fan, C.J., Li, J.L., Zhao, H., Lei, Y.B. (2011). Evaporative enrichment of oxygen-18 and deuterium in lake waters on the Tibetan Plateau. Journal of Paleolimnology, 46(2): 291-307.